arXiv:hep-ph/9608459v1 28 Aug 1996

Deep inelastic scattering on the deuteron in the Bethe-Salpeter formalism II: Realistic NN-interaction.

A.Yu. Umnikov [y] and F.C. Khanna
University of Alberta, Edmonton, Alberta T6G 2J1, Canada and TRIUMF, 4004 Wesbrook Mall, Vancouver, BC, Canada, V6T 2A3.

L.P. Kaptari
Bogoliubov Laboratory of Theoretical Physics, Joint Institute for Nuclear Research, Dubna, Russia.

(March 26, 2022)

25.30.-c, 13.60.Hb, 13.40.-f

We present a systematic study of the leading twist structure functions of the deuteron, F_2^D, $b_{1,2}^D$ and g_1^D in a fully relativistic approach. Our study is based on a realistic Bethe-Salpeter amplitude for the deuteron, which is obtained as a solution to the homogeneous Bethe-Salpeter equation with a realistic NN kernel. Particular effort is made to connect the structure functions to the densities of the appropriate charges and currents. This allows for a systematic comparison between the relativistic and nonrelativistic calculations, by analysing the same densities in both approaches. Thus, the sources of the relativistic effects in the structure functions are understood and clearly distinguished from variations caused by the differences in the model parameters. We present both the formalism and extensive numerical calculations for all steps of our analysis.

We find that the nonrelativistic and relativistic calculations are qualitatively very much alike. However, three main features systematically distinguish a consistent relativistic approach from the nonrelativistic one: (i) the binding effects are larger, (ii) the effect of Fermi motion at high x is stronger and (iii) the relativistic description of the structure functions $b_{1,2}^D$ is fully consistent, unlike the nonrelativistic approach, which is internally inconsistent and violates the fundamental sum rules.

I. INTRODUCTION

This paper is the second of the two papers devoted to a study of the deep inelastic lepton scattering (inclusive electroproduction) on the deuteron within the Bethe-Salpeter (BS) formalism. The first paper [1], presented a formal approach to the deep inelastic scattering within the BS formalism. The emphasize was on the self-consistency of the method, and the development of all aspects of the formalism so that it could be applied to a study of the realistic cases of reactions. Basic analysis was performed utilizing the operator product expansion method in the leading twist approximation. Subsequently, the results were obtained in

---

INFN Postdoctoral Fellow

[y] On leave from INFN, Sezione di Perugia and Department of Physics, University of Perugia, via A. Pascoli, Perugia, I-06100, Italy.

the space of the moments of the structure functions. Formal consistency of the approach was established and important sum rules were proven. However, all numerical estimates were performed in the "scalar deuteron" model which is rather far from reality. At the same time, it was stated that the following tasks have to be done in order to complete the study. First, explicit formulas for the deuteron spin-averaged and spin-dependent structure functions have to be derived, and, second, the structure functions have to be computed in a realistic meson-nucleon theory. The present paper deals with both of the tasks.

Utilizing the realistic BS amplitude of the deuteron, we calculate all the leading twist structure functions of the deuteron, and analyze the manifestations of the relativistic effects in these structure functions. Some of the preliminary results, including solution of the BS equation with realistic NN-interactions, were discussed previously [2–4]. However, this paper is not just a simple sum of results reported elsewhere, nor is it based solely on the direct application of the formalism developed in ref. [1], but rather presents a better understanding of the formal and physical aspects of the process.

It is imperative to mention now that in recent years a number of studies of the deep inelastic scattering of leptons off the deuteron have been done, referring to various manifestations of the relativistic features of the deuteron [5–10]. These studies certainly influenced our analysis during extensive studies in the time following the first publication [1]. Next, we found it convenient to use the formalism developed in refs. [11–13] in the late 1970-th (see also [14]). This formalism is more convenient if we deal with the structure functions, rather than the moments of structure functions (although it is mathematically equivalent, of course). Indeed, the formalism of ref. [1] allows us to calculate the physical moments of the structure functions using the deuteron amplitude under the Wick rotation. However, the numerical transform from the moments to the structure functions (the inverse Mellin transform) is not a well-defined operation. The new formalism allows for numerical treatment of the "inverse Wick rotation" of the Bethe-Salpeter amplitude of the deuteron for an application to the calculation of the structure functions.

Another new distinguishing feature of the present paper is the special accent on the systematic comparison of the relativistic and non-relativistic approaches. To do this, we consider a connection of the structure functions to the densities of appropriate charges and currents, and then analyze these densities in both relativistic and nonrelativistic approaches. In this way, we are able to trace the origins of the relativistic effects and demonstrate inconsistencies in the nonrelativistic approximations. The paper contains a number of illustrations for every step of our analysis.

Finally, results for the structure functions published previously have been recalculated using the new method and some of them have been corrected slightly.

The paper is organized as follows. In Section II, we define the densities of the currents which are used later in the analysis of the deep inelastic scattering. For this purpose, the realistic BS amplitude for the deuteron is presented, and the relativistic and nonrelativistic expressions for densities are defined and calculated within the realistic models. In Section III the relativistic formalism of the approach to the deep inelastic scattering on the deuteron is developed, including explicit relativistic and nonrelativistic formulae for the structure functions, and the sum rules for the structure functions are analyzed. Section IV contains results of the calculations of the structure functions F_2^D, $b_{1,2}^D$ and g_1^D in the realistic models, both relativistic and nonrelativistic. In Section V the summary of results of the paper is presented. Two Appendices contain important technical details.

II. ANATOMY OF THE DEUTERON

A. Realistic NN-interaction and Bethe-Salpeter amplitude

The basis of our approach to the relativistic description of the deep inelastic scattering o the deuteron is a nucleon-nucleon Bethe-Salpeter amplitude. General self-consistency of the approach has been analysed in our previous paper [1]. The way to construct relevant matrix elements has been shown and important sum rules have been proved, both without any reference to the particular model for the BS amplitude. A naive numerical estimate has been done within the scalar deuteron model which is found to be in a qualitative agreement with the nonrelativistic theory of the deep inelastic scattering [15{17].

Apparently, for the realistic calculations of the deuteron structure functions we need the realistic BS amplitude. The realistic BS amplitude of the deuteron is such an amplitude which provides us with a good description of bulk of the deuteron properties. This is the same ideology as it is in constructing the realistic wave function of the deuteron [18{22]. The most consistent way to obtain the realistic BS amplitude is to solve dynamical problem within the realistic model of the NN-interaction. The realistic NN-interaction still cannot be derived from the underlying fundamental theory, QCD, or its nonrelativistic approximations, such as the chiral perturbation theory. Although some progress has been achieved in recent years [23,24]. Alternatively, the parameters of the NN-interaction can be xed from the available experimental data on nucleon-nucleon scattering (phase shifts analysis), if the general form of interaction is somehow xed. This is a traditional way of action [18,19,25,22]. Unfortunately, the parametrization of the NN-interaction is dependent on the choice of a dynamical equation. In spite of certain similarity of the sets of parameters in all realistic models there is no universal potential for all nonrelativistic and relativistic potentials.

Only one parametrization of the NN-interaction is available for the BS equation, the parametrization of Fleischer and Tjon [25]. This parametrization is probably already due for a revision [26], incorporating new data on the nucleon-nucleon phase shift analysis [27]. However, this parametrization has been used as the basis for our recent calculation of the BS amplitude of the deuteron [2]. The meson parameters (masses, coupling constants, cut-o parameters) have been taken to be the same as in ref. [25,21], except for the coupling constant of the scalar -meson, which has been adjusted to provide a numerical solution of the homogeneous BS equation. The chosen set of meson parameters requires some minor adjustment, in view of two circumstances. First, here we use a simpli ed form of the propagator of the vector mesons, omitting $k\ k = {}^2_B$-term. Second, the di erent numerical procedures in solving the eigenvalue problem for the BS equation can also a ect the value of parameters.

A detailed formalism preceding the numerical solution of the BS equation for the deuteron is presented in ref. [1]. The Fredholm system of "Wick rotated" equations with all meson exchanges is solved by an iteration procedure with two dimensional gaussian integration (see e.g. ref. [28]). Eight components of the BS amplitude of the deuteron:

$$_{p1};\ \ {}^{0}_{a1};\ \ _{v1};\ \ _{a0};\ \ _{a2};\ \ {}^{0}_{t1};\ \ _{t0};\ \ _{t2}: \tag{2.1}$$

have been computed as scalar functions of two variables, p_0 and $|p|$. Now these components are available in the form of an analytical parametrization [29].

Since the one-boson exchange potential [21,25] was used only with a minor adjustment, our solution does not contain new physics (or different physics) than the pioneering paper. All parameters are presented in Table 1. The set of parameters includes the nucleon mass, m, the deuteron binding energy, ε_D, and, therefore, the deuteron mass, $M_D = 2m + \varepsilon_D$. The coupling constants are shown in accordance with our definition of the meson-nucleon form-factors:

$$F_B(k) = \frac{\Lambda^2 \quad \Lambda_B^2}{\Lambda^2 \quad k^2}; \tag{2.2}$$

where Λ is a cut-off parameter (see Table I).

B. Static properties and densities

In order to compare different models of the deuteron and define to what degree each of the models is realistic, it is natural to calculate various observables within these models and compare them with each other and with the experimental data. The canonical way to do this is to calculate the nucleon contributions to static observables, such as mean square radius, magnetic and quadrupole moments, etc. [18{22,30]. (The mesonic corrections are quite small and depend upon additional model assumptions.) Most of the modern realistic models give quite good description of the static properties, or have a decent explanation in the case of a minor discrepancy. The observables of the reactions, such as form factors and structure functions, are more model dependent. Those are often used as a tool for discriminating between models or certain ways of using models for calculations.

A direct comparison of the wave functions and amplitudes usually seems to be less meaningful. Still, in many cases particular properties of the wave functions and amplitudes directly indicate what will happen when observables are calculated. A good example here is the D-wave admixture, which directly affects values of the magnetic and quadrupole moments, tensor analysing power, T_{20}, and spin-dependent structure functions of the deuteron, g_1^D and b_2^D. Another example, the high momentum \tail" of the wave function (amplitude) dominates in the observables for some kinematic conditions with a high momentum transfer. However, the interpretation and properties of BS amplitudes are very different from the ones of the wave functions, a direct comparison between them is impossible.

Recently, it has been argued that a new intuition can be developed in working with the BS amplitude [30,29]. The approach is based on dealing with the charge and current densities. The same densities also can be calculated in the nonrelativistic approach with wave functions. Thus we gain a possibility to compare the models by comparing densities. Besides densities are more directly linked to the observables than wave functions and amplitudes. Following this guiding idea, we calculate the charge densities which are related to the various structure functions in deep inelastic scattering.

The nucleon contribution to the deuteron observable, $\hbar O i$, in many important cases is defined by the triangle diagram (see Fig. 1):

$$\hbar O i_M = i \int \frac{d^4p}{(2\pi)^4} \mathrm{Tr}^n \Lambda_M(p_0;p)\hat{O}(p_1;q;k)\Lambda_M(p_0+k_0;p+k)(\hat{p}_2 \quad m)^o; \tag{2.3}$$

where $p_{1;2} = P_D = 2 \quad p = (M_D = 2 \quad p_0; \quad p)$, $P_D = (M_D;0)$ is the deuteron momentum in the rest frame, $p = (p_0;p)$ is the relative momentum of nucleons, $\hat{O}(p_1;q;k)$ is an appropriate operator and $\Lambda_M(p_0;p)$ is the

Bethe-Salpeter amplitude for the deuteron with M being the deuteron's total angular momentum projection (see Ref. [1] for definition and conventions for $_M(p_0;p)$). The operator $\hat{O}(p_1;q;k)$ is written in a general form, depending on nucleon momentum, p_1 and two external momenta, q which does not sneak into the lower part of the diagram and k which adds to nucleon momentum. In the present paper we consider only the case with $k = 0$.

The explicit form of operators and structure of the deuteron matrix elements relevant to the deep inelastic scattering, were studied previously [16,17,5{7,1]. One of the methods to find a form of the operator for deep inelastic scattering is to adopt the Wilson's Operator Product Expansion [31] and use it within the effective meson nucleon theory [16,17,32,1]. Other possible approach is based on a parametrization of the operators in the most general form with analysis of all structures phenomenologically or within models for quark-nucleon amplitudes [5{7,14,33]. Both approaches lead to the same results in "convolution approximation" which assumes that the deformation of the nucleon operator off-mass-shell can be neglected. Very small and strongly model dependent corrections to the convolution are qualitatively similar in both approaches. In the present paper we do not concentrate on the differences between these two approaches, i.e. our analysis is not going beyond the convolution approximation.

Thus, the relevant operators are vector, $$, and axial vector, $_5$. Let us define the matrix elements of the following components of these operators:

$$\begin{pmatrix} h\ _0 i_M \\ h\ _3 i_M \\ h\ _5\ _0 i_M \\ h\ _5\ _3 i_M \end{pmatrix} = \frac{i}{2M_D}\int \frac{d^4p}{(2\ )^4}\mathrm{Tr}\ \ _M(p_0;p)\begin{pmatrix} _0 \\ _3 \\ _5\ _0 \\ _5\ _3 \end{pmatrix}\ _M(p_0;p)(\hat{p}_2\quad m)\ ; \tag{2.4}$$

where notation in the l.h.s. are obvious and we use this notation in what follows. There are three main combinations of these matrix elements which are important for deep inelastic scattering and which are discussed in the present paper. They are presented below together with the correspondent structure functions of the deuteron:

$$F_2^D \quad ! \quad \frac{1}{3}\sum_M \ fh\ _0 i_M + h\ _3 i_M g \tag{2.5}$$

$$b_2^D \quad ! \quad fh\ _0 i_{M=1} + h\ _3 i_{M=1} g \quad fh_0 i_{M=0} + h\ _3 i_{M=0} g \tag{2.6}$$

$$g_1^D \quad ! \quad fh\ _5\ _0 i_{M=1} + h\ _5\ _3 i_{M=1} g; \tag{2.7}$$

where ! means "corresponding to" and does not have a direct mathematical interpretation. Explicit connection of these matrix elements to the structure functions will be discussed in Section III. The important circumstance now is that these matrix elements present charges and currents, vector and axial vector, calculated for the deuteron states with different combinations of the total angular momentum projections, M. Properties of these matrix elements, including rigorous sum rules for the charges, are used later to discuss the structure functions.

Let us start from the matrix elements involved in eq. (2.5). The first term, $h\ _0 i_M$, is the charge of the conserved vector current and since it is independent of M the following sum rules can be immediately written down (see e.g. [16,1]):

$$\frac{1}{3}\sum_M \langle \Gamma_0\rangle_M = \langle \Gamma_0\rangle_M = 1: \tag{2.8}$$

Obviously this sum rule is also valid in the nonrelativistic approaches, since it is just a normalization condition for both the wave functions and BS amplitudes. To make more meaningful use of this matrix element and compare our approach to other realistic approaches, we define charge density in the BS formalism as (see Appendix A for explicit form):

$$\langle \Gamma_0\rangle^{BS}(p) = \frac{i}{12\pi^2 M_D}\sum_M \int \frac{dp_0}{2\pi}\mathrm{Tr}\ \Phi_M(p_0;p)\,\Gamma_0\,\Phi_M(p_0;p)(\hat{p}_2 - m)\ ; \tag{2.9}$$

$$\frac{1}{4}\int dp\,\langle \Gamma_0\rangle^{BS}(p) = 1; \tag{2.10}$$

which in the nonrelativistic limit corresponds to the momentum density [17,1,8]:

$$\langle \Gamma_0\rangle^{NR}(p) = \frac{1}{6\pi^2}\sum_M |\psi_M(p)|^2 = u^2(|p|) + w^2(|p|)\ ; \tag{2.11}$$

$$\frac{1}{4}\int dp\,\langle \Gamma_0\rangle^{NR}(p) = 1; \tag{2.12}$$

where $\psi_M(p)$ is a nonrelativistic wave function of the deuteron (do not confuse with the Bethe-Salpeter amplitude, $\Phi_M(p_0;p)$!) with u and w being its S-and D-wave components. The densities, $\langle \Gamma_0\rangle(p)$, calculated in three realistic models [18,19,2] are shown in Fig. 2 as functions of $|p|$. Certain model differences at $|p| > 0.5$ GeV are present, however there is no distinguishing feature of the relativistic density.

Similarly, we consider other components of the vector and axial matrix elements. The relativistic densities, $\langle \Gamma_3\rangle^{BS}(p)$, $\langle \Gamma_5\Gamma_0\rangle^{BS}(p)$, etc, are defined by replacing Γ_0 with Γ_3, $\Gamma_5\Gamma_0$, etc, and taking appropriate combination of the matrix elements with different M in eq. (2.9). The explicit expressions for all densities in terms of components of the BS amplitude are presented in the Appendix A.

The nonrelativistic densities are calculated using methods of nonrelativistic reduction [17,1,8]. Here we present the most interesting of them. A remarkable feature of the non-relativistic densities is that they have the same angular dependences as the corresponding relativistic densities.

The 3rd spatial component of the vector current in the nonrelativistic limit gives:

$$\langle \Gamma_3\rangle^{NR}(p) = \frac{p_3}{6\pi^2 m}\sum_M |\psi_M(p)|^2 + O\left(\frac{|p|^3}{m^3}\right) \sim \frac{|p|\cos\theta}{m}\,u^2(|p|) + w^2(|p|)\ ; \tag{2.13}$$

where θ is polar angle of vector p. Note, this density has a suppression factor of $|p|/m$, due to a mixing of upper and lower components of the Dirac spinors by non-diagonal matrix Γ_3. Since the angular dependence of the explicit form of the relativistic density $\langle \Gamma_3\rangle^{BS}(p)$ is also absorbed in the factor $\cos\theta$ (see Appendix A), the integrals of both relativistic and nonrelativistic densities $\langle \Gamma_3\rangle$ over dp are zero:

$$\int dp\,\langle \Gamma_3\rangle^{BS}(p) = \int dp\,\langle \Gamma_3\rangle^{NR}(p) = \langle \Gamma_3\rangle \sim \int_{-1}^{1} d(\cos\theta)\cos\theta = 0; \tag{2.14}$$

These densities for realistic models are show in Fig. 3 at $\theta = 0$. Basically they just reflect the behavior of the charge densities from Fig. 2 in accordance with the nonrelativistic formula (2.13). For illustration, the curve representing the BS density from Fig. 2 multiplied by the factor $|p|/m$ is also shown (dash-dotted).

Surprisingly enough, it barely can be distinguished from the exact $h_3 i^{BS}(p)$ (solid line) even at momenta higher than m.

Two examples of spin-dependent densities:

$$h_0 i^{NR}_{M=1}(p) \quad h_0 i^{NR}_{M=0}(p) \sim \frac{3}{2} P_2(\cos\theta) w(|p|) \quad 2^{\sqrt{2}} u(|p|) + w(|p|) \quad ; \tag{2.15}$$

$$h_5 \quad {}_3 i^{NR}_{M=1}(p) \sim u^2(|p|) \quad \frac{1}{2} w^2(|p|) + P_2(\cos\theta) w(|p|) \quad w(|p|) \quad {}^{\sqrt{2}} u(|p|) \quad ; \tag{2.16}$$

where $P_2(x)$ is the Legendre polynomial. We also can easily write down sum rules for the spin-dependent densities (2.15) and (2.16):

$$\int dp \quad h_0 i^{NR}_{M=1}(p) \quad h_0 i^{NR}_{M=0}(p) \quad / \quad \int_{1}^{1} d(\cos\theta) P_2(\cos\theta) = 0; \tag{2.17}$$

$$\frac{1}{4} \int dp h_5 \quad {}_3 i^{NR}(p) = 1 \quad \frac{3}{2} w_D \; ; \tag{2.18}$$

where w_D is the weight of the D-wave in the deuteron. The relativistic analogue of the sum rule (2.18) can be used for an estimate of the "admixture" of the D-wave in the relativistic formalism which otherwise does not allow for probabilistic interpretation. Numerically we have:

$$\frac{1}{4} \int dp h_5 \quad {}_3 i^{BS}(p) \sim 0.9215; \tag{2.19}$$

which gives us an estimate of $w_D \quad 5\%$ [1].

The realistic model densities (2.15) and (2.16) are presented in Figs. 4 and 5, respectively. These two examples confirm the conclusions of the previous illustrations: (i) realistic models are in a reasonable agreement among each other, providing description of the charge and current densities of the deuteron, and (ii) in spite of some model variations at high momentum, there is no distinguishing feature of the densities obtained in a relativistic BS formalism. Therefore, we can not expect striking relativistic effects caused by the form of the densities. However, this conclusion does not close a possibility for effects generated by the differences in the relativistic and non-relativistic description of the deep inelastic reaction.

III. RELATIVISTIC THEORY OF THE DEEP INELASTIC SCATTERING ON THE DEUTERON

A. Definitions and kinematics

We start with the general form of the hadronic tensor of the deuteron with the total angular momentum projection, M, keeping only leading twist structure functions:

---

[1] There can be corrections, $O(|p|^2/m^2)$, to the density, $h_5 \quad {}_3 i^{NR}_{M=1}(p)$, see refs. [32,8]. However, their estimated contribution to integral (2.18) is small, $< 1\%$.

$$W^D(q;P_D;M) = \quad g + \frac{q\,q}{q^2} F_1^D(x_D;Q^2;M) + P_D \quad q\frac{P_D q}{q^2} \quad P_D \quad q\frac{P_D q}{q^2} \frac{F_2^D(x_D;Q^2;M)}{P_D q}$$
$$+ \frac{iM_D}{P_D q} \quad q\, S_D(M) g_1^D(x_D;Q^2); \tag{3.1}$$

where $q = (;0;0; \quad \overline{{}^2 + Q^2})$ is the momentum transfer, $Q^2 = \quad q^2$, $x_D = Q^2 = (2P_D q)$ (in the rest frame of the deuteron $x_D = Q^2 = (2M_D \quad))$, $S_D(M)$ is the deuteron spin (see Appendix B) and $F_{1;2}^D$ and g_1^D are the deuteron structure functions. Averaged over the M this expression leads to the well-known form of the spin-independent hadronic tensor which is valid for hadrons with any spin:

$$W^D(q;P_D) = \frac{1}{3}\sum_M W^D(q;P_D;M) \tag{3.2}$$

$$= \quad g + \frac{q\,q}{q^2} F_1^D(x_D;Q^2) + P_D \quad q\frac{P_D q}{q^2} \quad P_D \quad q\frac{P_D q}{q^2} \frac{F_2^D(x_D;Q^2)}{P_D q}; \tag{3.3}$$

where $F_{1;2}^D(x_D;Q^2)$ are result of averaging of the SF $F_{1;2}^D(x_D;Q^2;M)$. It is easy to nd that other structure functions can be obtained as a result of other combinations of $W^D(q;P_D;M)$ with di erent M :

$$W^D(q;P_D;M = 1) \quad W^D(q;P_D;M = \quad 1) \,/\, g_1^D(x_D;Q^2); \tag{3.4}$$

$$W^D(q;P_D;M = 1) \quad W^D(q;P_D;M = 0) \,/\, b_{1;2}^D(x_D;Q^2) \tag{3.5}$$

The eqs. (3.2), (3.4) and (3.5) are the basis for the experimental measurements of the deuteron structure functions. However, for the purpose of theoretical studies of the hadronic tensor and structure functions the projection technique is more convenient. All relevant formulae for projection technique are presented in Appendix B. More background information on the SF $b_{1;2}^D$ can be found in refs. [34{37].

To calculate the hadronic tensor of the deuteron we follow the general formalism of our approach:

$$W^D(q;P_D;M) = i\sum \frac{d^4p}{(2\ )^4} \mathrm{Tr}\,{}^n{}_M(p_0;p)\hat{W}^N(p_1;q)\ {}_M(p_0;p)(\hat{p}_2 \quad m)^o; \tag{3.6}$$

The nucleon tensor operator, $\hat{W}^N(q;p)$, has been studied extensively in recent years [16,32,1,5,6,8,14]. We use a well established form of the operator, leading to the convolution formula [38]:

$$\hat{W}^N(q;p) = \hat{W}_{f\quad g}(q;p) + \hat{W}_{[\quad]}(q;p) \tag{3.7}$$

$$\hat{W}_{f\quad g}(q;p) = \frac{\hat{q}}{2pq} W^N(q;p); \tag{3.8}$$

$$\hat{W}_{[\quad]}(q;p) = \frac{i}{2pq} \quad q \quad {}_5 g_1^N(q;p); \tag{3.9}$$

where f:::g and [:::] denote symmetrization and antisymmetrization of indices, respectively, and $g_1^N(q;p) = g_1^N(x;Q^2)$ is the spin-dependent nucleon SF. The hadronic tensor of the nucleon, $W \quad (p;q)^N$, is de ned as:

$$W^N(q;p) = \quad g + \frac{q\,q}{q^2} F_1^N(x;Q^2) + p \quad q\frac{pq}{q^2} \quad p \quad q\frac{pq}{q^2} \frac{F_2^N(x;Q^2)}{pq}; \tag{3.10}$$

where $x = Q^2 = (2pq)$ and $F_{1;2}^N$ are the nucleon SFs. The small e ects of the o -mass-shell deformation of the nucleon tensor [5,8,39] are not considered here, since these e ects do not a ect sum rules for SF and do not

noticeably change the absolute values of the SFs. That is why SFs $F^N_{1;2}$ in (3.10) do not depend on p^2, but q^2 and pq.

Using projectors (Appendix B), we extract SFs from the hadronic tensor of the deuteron:

$$F_1^D(x_N;Q^2;M) = i\int\frac{d^4p}{(2\ )^4}F_1^N\left(\frac{x_N m}{p_{10}+p_{13}};Q^2\right)\frac{\mathrm{Tr}\ {}_M(p_0;p)(\ {}_0+\ {}_3)\ {}_M(p_0;p)(\hat{p}_2\quad m)}{2(p_{10}+p_{13})}; \tag{3.11}$$

$$F_2^D(x_N;Q^2;M) = i\int\frac{d^4p}{(2\ )^4}F_2^N\left(\frac{x_N m}{p_{10}+p_{13}};Q^2\right)\frac{\mathrm{Tr}\ {}_M(p_0;p)(\ {}_0+\ {}_3)\ {}_M(p_0;p)(\hat{p}_2\quad m)}{2M_D}; \tag{3.12}$$

$$g_1^D(x_N;Q^2) = i\int\frac{d^4p}{(2\ )^4}g_1^N\left(\frac{x_N m}{p_{10}+p_{13}};Q^2\right)\frac{\mathrm{Tr}\ {}_M(p_0;p)(\ {}_0+\ {}_3)\ {}_5\ {}_M(p_0;p)(\hat{p}_2\quad m)\ {}_{M=1}}{2(p_{10}+p_{13})}; \tag{3.13}$$

where $x_N = Q^2/(2m\ )$ is the Bjorken scaling variable[2], i.e. this is x for the on-mass-shell nucleon at rest, p_{10} and p_{13} are the time and 3-rd components of the struck nucleon momentum. Formulas (3.11) and (3.12) have not been averaged over the projection M since in the present form it gives an understanding of the SF $b^D_{1;2}$. Indeed, for instance eq. (3.12) gives two independent "SFs", with $M = \quad 1$ and $M = 0$, which are related to the usual spin-independent SF, F_2^D, and a new SF, b_2^D:

$$F_2^D(x_N;Q^2) = \frac{1}{3}\sum_{M=0;\ 1}F_2^D(x_N;Q^2;M); \tag{3.14}$$

$$b_2(x_N;Q^2) = F_2^D(x;Q^2;M = +1)\quad F_2^D(x;Q^2;M = 0); \tag{3.15}$$

$$F_2^D(x_N;Q^2;M = +1) = F_2^D(x_N;Q^2;M = \quad 1): \tag{3.16}$$

Note, the SF $F_2^D(x;Q^2;M)$ is independent of the lepton polarization, therefore, both SFs, F_2^D and b_2^D, can be measured in experiments with an unpolarized lepton beam and polarized deuteron target. In view of eq. (3.16), only one of the SFs $F_2^D(x;Q^2;M)$ is needed, in addition to the spin-independent $F_2^D(x;Q^2)$, in order to obtain $b_2(x;Q^2)$. The other SF, b_1^D, is related to the deuteron SF F_1^D, the same way as b_2^D is related to F_2^D, viz. via eqs. (3.14), and $b_2^D = 2xb_1^D$.

B. Singularities of the triangle diagram and calculation of structure functions

It has been shown previously [11{14] how a singular structure of the triangle graph (Fig. 1) rules the behavior of the spin-independent SF F_2^D. In particular, it is found that the relativistic impulse approximation satis es the unitarity and provides the correct kinematical region of the variable x_N. However, both these properties of the exact covariant amplitude are violated in practical calculations, when nonrelativistic wave functions of the deuteron are used. In this case one can refer to the argument that such deviations are small, and are not important for phenomenology. At the same time, a realistic Bethe-Salpeter amplitude of the deuteron serves ideally for a consistent phenomenological application of the covariant theory of the processes on the bound nucleons.

---

[2] Note that the "native" deuteron variable is $x_D = (m/M_D)x_N$, however x_N is used more often.

In order to calculate SFs, (3.12)–(3.15) and analyze the sum rules, the singularities of the triangle diagram should be explicitly taken into account. To do that, eq. (3.12) is rewritten as:

$$F_2^D(x_N;Q^2;M) = \frac{i}{2M_D}\int \frac{d^4p}{(2\pi)^4} F_2^N\left(\frac{x_N m}{p_{10}+p_{13}};Q^2\right)$$
$$\frac{1}{(p_1^2-m^2+i\varepsilon)^2(p_2^2-m^2+i\varepsilon)}\mathrm{Tr}\,\Gamma_M(p_0;p)(\hat{p}_1+m)(\gamma_0+\gamma_3)(\hat{p}_1+m)\Gamma_M(p_0;p)(\hat{p}_2+m)\,; \qquad (3.17)$$

where $\Gamma_M(p_0;p) = (\hat{p}_1-m)\Gamma_M(p_0;p)(\hat{p}_2-m)$ is the Bethe-Salpeter vertex function of the deuteron.

Analysis of singularities in the complex p_{2+}-plane allows for one analytical integration in (3.17) [13]. After translation into variables which are used in the present paper, this integration is equivalent to picking the residue of the second nucleon pole, $p_{20} = \omega = \sqrt{m^2+p^2}$ or $p_0 = M_D/2 - \omega$, in the complex p_0-plane when both of the following conditions are satisfied:

$$0 < \omega - p_3 < M_D\,: \qquad (3.18)$$

The contribution of the region of p beyond (3.18), to the integral (3.17), is zero, i.e. different poles cancel each other. Note, that $p_{10} = M_D - \omega$ in the required pole. Calculating residue in (3.17), one gets:

$$F_2^D(x_N;Q^2;M) = \frac{1}{2M_D}\int \frac{d^3p}{(2\pi)^3} F_2^N\left(\frac{x_N m}{M_D-\omega+p_3};Q^2\right)\theta(M_D-\omega+p_3) \qquad (3.19)$$
$$\frac{1}{2\omega M_D^2(M_D-2\omega)^2}\mathrm{Tr}\,\Gamma_M(p_0;p)(\hat{p}_1+m)(\gamma_0+\gamma_3)(\hat{p}_1+m)\Gamma_M(p_0;p)(\hat{p}_2+m)\Big|_{p_0=\frac{M_D}{2}-\omega}\,;$$

where the θ-function guaranties the right of conditions (3.18) is satisfied, and the left condition is always satisfied.

It is useful to rewrite (3.19) in the convolution form:

$$F_2^D(x_N;Q^2;M) = \int_{x_N}^{M_D/m} dy\, F_2^N\left(\frac{x_N}{y};Q^2\right) f_M^{N/D}(y); \qquad (3.20)$$

where "the effective distribution" of nucleons in the deuteron is defined by

$$f_M^{N/D}(y) = \frac{1}{2M_D}\int \frac{d^3p}{(2\pi)^3}\, y\,\frac{M_D-\omega+p_3}{m}\,\theta(y)\,\frac{1}{2\omega M_D^2(M_D-2\omega)^2} \qquad (3.21)$$
$$\mathrm{Tr}\,\Gamma_M(p_0;p)(\hat{p}_1+m)(\gamma_0+\gamma_3)(\hat{p}_1+m)\Gamma_M(p_0;p)(\hat{p}_2+m)\Big|_{p_0=\frac{M_D}{2}-\omega}\,:$$

The SFs $F_{1;2}^D$ and $b_{1;2}^D$ are now calculated as follows:

$$\begin{pmatrix} F_1^D(x_N;Q^2) \\ b_1^D(x_N;Q^2) \end{pmatrix} = \int_{x_N}^{M_D/m}\frac{dy}{y}\begin{pmatrix} f^{N/D}(y) \\ \tilde{f}^{N/D}(y) \end{pmatrix} F_1^N\left(\frac{x_N}{y};Q^2\right)\,; \qquad (3.22)$$

$$\begin{pmatrix} F_2^D(x_N;Q^2) \\ b_2^D(x_N;Q^2) \end{pmatrix} = \int_{x_N}^{M_D/m} dy \begin{pmatrix} f^{N/D}(y) \\ \tilde{f}^{N/D}(y) \end{pmatrix} F_2^N\left(\frac{x_N}{y};Q^2\right)\,; \qquad (3.23)$$

where distributions $f^{N/D}$ and $\tilde{f}^{N/D}$ are given by

$$f^{N=D}(y) = \frac{1}{3}\sum_M f_M^{N=D}(y); \tag{3.24}$$

$$f^{N=D}(y) = f_1^{N=D}(y) \quad f_0^{N=D}(y): \tag{3.25}$$

Similarly, for the SF g_1^D we get:

$$g_1^D(x_N;Q^2) = \int_{x_N}^{M_D=m} \frac{dy}{y} g_1^N\left(\frac{x_N}{y};Q^2\right) f^{N=D}(y); \tag{3.26}$$

where the effective polarized distribution of nucleons in the deuteron is defined by

$$f^{N=D}(y) = \frac{1}{2M_D}\int \frac{d^3p}{(2\ )^3}\ y\ \frac{M_D\ \ w + p_3}{m}\ (y)\ \frac{1}{2!M_D^2(M_D\ \ 2!)^2} \tag{3.27}$$

$$\mathrm{Tr}\ {}_{M=1}(p_0;p)(\hat{p}_1+m)(\ {}_0+\ {}_3)\ {}_5(\hat{p}_1+m)\ {}_{M=1}(p_0;p)(\hat{p}_2+m)\ {}_{p_0=\frac{M_D}{2}}\ !$$

C. Sum rules for the deuteron structure functions

Two sum rules can be written for the effective distribution $f_M^{N=D}(y)$:

$$\int_0^{M_D=m} f_M^{N=D}(y)dy = \frac{1}{4}\int dp\, h\ {}_0 i_M\ (p) = h\ {}_0 i_M\ = 1; \tag{3.28}$$

$$\int_0^{M_D=m} y f_M^{N=D}(y)dy = hD\,j(\ {}_N)\ \ jD\,i_M\ = 1\ \ {}_N; \tag{3.29}$$

where $(\ {}_N)\ /\ i\ (x)\ \ @\ \ (x)$ is the trace of the energy-momentum tensor. Eq. (3.28) presents the vector charge conservation generalized for the deuteron states with different M (see eqs. (2.9)–(2.10)). In spite of clear physical interpretation, some time ago it was a subject of some controversy [11{13]. Indeed, the derivation of sum rule (3.28) contains some subtle points and equivalence between it and the expression for the charge, (2.8), is a non-trivial fact, particularly, because of the presence of the -function in eq. (3.21). This -function provides correct kinematics in variable x_N but cuts out a part of the integration domain in d^3p. This cutting of the integration interval in the polar angle leads to non-zero contribution of the matrix element containing ${}_3$, which is proportional to cos . However, the validity of this sum rule has been firmly established [11{13]. The sum rule (3.29) for the first moment of $f_M^{N=D}$ is of a different nature, it presents the nucleon contribution to the total momentum of the deuteron [16,40,17,1] and ${}_N$ is a part of the total momentum carried by the non-nucleon component (mesons). The constant ${}_N$ cam not be fixed in a model independent fashion, rather it is calculated within any particular model. Self-consistency of the theory requires that meson exchange current contribution into the deuteron SF, F_2^D, exactly compensates the loss of energy by nucleons, (3.29). An important property of sum rules, (3.28) and (3.29), is that their r.h.s. does not depend on the deuteron spin orientation.

The sum rules for $f^{N=D}(y)$ and $f^{N=D}(y)$ follow from sum rules for $f_M^{N=D}(y)$ and definitions (3.24)–(3.25):

$$\int_0^{M_Z=m} f^{N=D}(y)dy = \frac{1}{3}\sum_M h_0 i_M = h_0 i = 1; \tag{3.30}$$

$$\int_0^{M_Z=m} y f^{N=D}(y)dy = \frac{1}{3}\sum_M h_D j(\ _N)\ j_D i_M = 1\ _N; \tag{3.31}$$

$$\int_0^{M_Z=m} f^{N=D}(y)dy = h_0 i_{M=1} \quad h_0 i_{M=0} = 0; \tag{3.32}$$

$$\int_0^{M_Z=m} y\ f^{N=D}(y)dy = h_D j(\ _N)\ j_D i_{M=1} \quad h_D j(\ _N)\ j_D i_{M=0} = 0: \tag{3.33}$$

Sum rules for the deuteron SFs b_1^D and b_2^D are the immediate result of combining eqs. (3.32)–(3.33) and (3.22)–(3.23):

$$\int_0^1 dx_D\, b_1^D(x_D) = 0; \tag{3.34}$$

$$\int_0^1 dx_D\, b_2^D(x_D) = 0; \tag{3.35}$$

in an agreement with the sum rules suggested by Efremov and Teryaev [34].

Sum rule for the spin-dependent distribution relates the integral of the spin-dependent distribution of nucleons to the 3-rd component of the axial current, (2.19):

$$\int_0^{M_Z=m} f^{N=D}(y)dy = h_5\ {}_3 i^{BS}_{M=1}: \tag{3.36}$$

An explicit expression for the distribution function $f_M^{N=D}(y)$ (and therefore of $f^{N=D}(y)$ and $f^{N=D}(y)$) in terms of the components of the Bethe-Salpeter amplitude can be directly established from eqs. (3.21) and (3.27) and formulae for the corresponding densities are given in Appendix A.

D. Calculation of distributions: Inverse Wick rotation.

To calculate numerically the effective distribution functions, (3.21), (3.24), (3.25) and (3.27), we need to know the matrix elements over the BS vertex functions as functions of p and at $p_0 = M_D = 2\sqrt{m^2 + p^2}$ along real p_0. Let us remind that the components of BS amplitude have been found along imaginary axis in p_0-plane (Wick rotation).

We explain the procedure of calculating the \inverse Wick rotated" matrix element using an example of $f^{N=D}(y)$. Other distributions are calculated the same way. First, let us rewrite eq. (3.21) in the form:

$$f^{N=D}(y) = \frac{1}{2M_D}\int \frac{d^3p}{(2\ )^3}\ y\ \frac{M_D\ \ w + p_3}{m}\ (y)\ \ h_0 i^{BS}_{pole}(p) + h_3 i^{BS}_{pole}(p)\ ; \tag{3.37}$$

where $h\,{}_0 i^{BS}_{pole}(p)$ and $h\,{}_3 i^{BS}_{pole}(p)$ are the densities defined similarly to eq. (2.9), but in the "pole approximation", i.e. exact integral is replaced by residue at the second nucleon pole. An explicit form of $h\,{}_0 i^{BS}_{pole}(p)$ and $h\,{}_3 i^{BS}_{pole}(p)$ is clear from eqs. (3.21) and (3.37). Second, we notice that this density does not have any singularities in the complex plane of p_0. Neither does the matrix element:

$$\begin{aligned} &\mathrm{Tr}\ {}_M(p_0;p)(\hat{p}_1+m)({}_0+{}_3)(\hat{p}_1+m)\,{}_M(p_0;p)(\hat{p}_2+m) \\ &= (p_1^2-m^2)^2(p_2^2-m^2)\mathrm{Tr}\ {}_M(p_0;p)({}_0+{}_3)\,{}_M(p_0;p)(\hat{p}_2-m)\ : \end{aligned} \tag{3.38}$$

Therefore, to calculate the density in the pole approximation, the matrix element (3.38) can be safely expanded into a Taylor series in the variable p_0 around the point $p_0 = 0$. Third, the coefficients of the Taylor expansion can be calculated, using the known r.h.s. of eq. (3.38) along imaginary p_0. And last, a convergence of the expansion can be checked numerically, by comparing results of calculations up to different order in p_0. Note, that eq. (3.38) and similar expressions for all other distributions are even functions of p_0, therefore the Taylor expansion really should be done in p_0^2. In addition, the point $p_0 = 0$ should be a good point for the Taylor expansion, since in the most physically interesting region of $|p|/m \quad 1$ we have $|p_0/m| \quad \varepsilon_D/(2m) \quad |p|^2/(2m^2) \quad 1$. The critical point for any expansion in the nuclear physics is usually $|p|/m = 1$. However, even at this point $|p_0/m|$ is still a good parameter for the Taylor expansion, $|p_0/m| \quad \varepsilon_D/(2m) \quad (\sqrt{2} \quad 1) \quad 0.4$. Parameter $|p_0/m|$ is getting close to 1, with $|p|/m \quad 1.5$.

The results of calculations of the charge density in the pole approximation, $h\,{}_0 i_{pole}(p)$, are presented in Fig. 6, where we compare curves for calculations up to p_0^0, p_0^2 and p_0^4. As we expected, the procedure is nicely convergent up to $|p| \quad 1$ GeV and with reasonable accuracy can be used up to $|p| \quad 1.5$ GeV. Similar results for the axial density in pole approximation, $h\,{}_5\,{}_3 i_{pole}(p)$, are shown in Fig. 7.

Note, the numerical approximation made in this section, such as limiting number of terms in the Taylor expansion, can potentially cause a violation of the exact sum rules.

E. Nonrelativistic formulae for structure functions

The nonrelativistic expressions for $f^{N=D}(y)$, $f^{N=D}(y)$ and $f^{N=D}(y)$ can be obtained by using an analogy of the charge densities calculated within the Bethe-Salpeter formalism and corresponding densities calculated with wave functions (e.g. (2.11), (2.13), (2.15) and (2.16)). Actually, the distributions in the BS formalism are expressed in terms of densities in the nucleon pole approximation, (3.21), (3.25) and (3.27) and not exact densities as (2.9). However, one can hope that the nucleon pole contribution gives the main contribution to the density, at least in the non-relativistic region. Such type of assumption is very common for nuclear physics (see e.g. [20,22,41,6,7]). For instance, the well-known result for the spin-independent distribution is immediately reproduced (see e.g. [17,14,16]):

$$\begin{aligned} f^{N=D}_{NR}(y) &= \int \frac{d^3p}{(2\ )^3}\ \ y\ \ \frac{M_D\ \ w+p_3}{m}\ \ (y)\ \ h\,{}_0 i^{NR}(p) + h\,{}_3 i^{NR}(p) \\ &= \int \frac{d^3p}{(2\ )^3}\ \ y\ \ \frac{M_D\ \ w+p_3}{m}\ \ (y)\,(1+\frac{|p|\cos}{m})\ \ u^2(|p|)+w^2(|p|)\ : \end{aligned} \tag{3.39}$$

The presence of the $\ $-function on the r.h.s. of eq. (3.39) slightly violates the sum rule (3.30). However, this is not noticeable phenomenologically, since the only region of large momenta, $|p| > 0.7$ GeV, is affected by

the -function and it does not contribute much to the norm of the deuteron wave function. We can accept such slight effect of the -functions, since a nonrelativistic approximation is based on the belief that high momenta are not important and if something is wrong there we just ignore it.

For distribution $f^{N=D}(y)$, we get:

$$f^{N=D}_{NR}(y) = \int \frac{d^3p}{(2\ )^3}\ y\ \frac{M_D\ w + p_3}{m}\ (y) \tag{3.40}$$

$$(1 + \frac{jp\,j\cos}{m})P_2(\cos\ )\frac{3}{2}w(jp\,j)^n\ 2^p\ \bar{2}u(jp\,j) + w(jp\,j)^o\ :$$

Again, the sum rule (3.32) is broken by the presence of the -function in (3.40). Neglecting it, one gets

$$\int_0^1 dx_D\, b_1^D(x_D) \Big/ \int_0^{M_D/2=m} f^{N=D}_{NR}(y)dy$$

$$\Big/ \int_1^1 d(\cos\ )(1 + \frac{jp\,j\cos}{m})P_2(\cos\ ) = 0; \tag{3.41}$$

where the orthogonality property of the Legendre polynomials is used.

A deviation from zero, caused by the -functions is not large compared to 1, but anything is large compare to 0! One can artificially adjust formula (3.40) to fulfill this sum rule. For instance, small corrections to the normalization of both terms with M = 1 and M = 0 can be made to satisfy the sum rule in the form (3.32). However, the situation with the second sum rule, (3.35) and (3.42), is more difficult and can not be fixed by any simple adjustments of the normalizations or ignoring the functions. Similar to eq. (3.41), it can be written (neglecting the -function!) as:

$$\int_0^1 dx_D\, b_2^D(x_D) \Big/ \int_0^{M_D/2=m} y\ f^{N=D}_{NR}(y)dy$$

$$\Big/ \int_1^1 d(\cos\ )(M_D\ w + jp\,j\cos\ )(1 + \frac{jp\,j\cos}{m})P_2(\cos\ ) \neq 0: \tag{3.42}$$

Thus, there is no reason for this sum rule to be satisfied with the nonrelativistic distribution function (3.40). Therefore the nonrelativistic formulae, in principle, violates the sum rules for the SFs $b^D_{1;2}$. However, we can still hope that it will be a small effect, one not noticeable in practice.

Nonrelativistic formulae for other spin-dependent distribution, $f^{N=D}$, are also a straightforward result of using density (2.16) instead of the relativistic density in the pole approximation in eq. (3.27) (see also footnote to the formula (2.19)):

$$f^{N=D}_{NR}(y) = \int \frac{d^3p}{(2\ )^3}\ y\ \frac{M_D\ w + p_3}{m}\ (y) \tag{3.43}$$

$$u^2(jp\,j)\ \frac{1}{2}w^2(jp\,j) + P_2(\cos\#)w(jp\,j)\ w(jp\,j)\ \ {}^p\bar{2}u(jp\,j)\ :$$

and the sum rule follows from eq. (2.18):

$$\int_0^{M_D/m} f_{NR}^{N=D}(y)dy = 1 - \frac{3}{2}w_D \tag{3.44}$$

F. Calculation of distributions: relativistic vs. nonrelativistic

In order to understand if relativistic distribution functions, (3.21), (3.25) and (3.27), are significantly different from the nonrelativistic distributions, (3.39), (3.40) and (3.27), we have to understand fully an effect of the one pole approximation on the densities in the BS formalism. Indeed, discussion of Section IIB prepared us to the fact that we can not expect significant physical effects from the form of the densities, since both relativistic and nonrelativistic realistic models lead to similar results and we do not detect any special trend for the relativistic model.

In Figs. 8 and 9 we compare the exact densities and densities in the one pole approximation, for two most important densities h_0 and $h_{5\ 3}$. We find that one pole approximation leads to a significant change in the density. The densities in one pole approximation (solid curves) have much harder tail compared to the exact densities (dotted curves), starting at $|p| \quad 0.5m$, and effect is an order of magnitude at $|p| \quad 1.5m$. This can be qualitatively understood, considering an example of the charge density, h_0. Indeed, picking the nucleon pole in the full integral, corresponds to neglecting the antinucleon (negative) contribution to total charge density which concentrates at high momenta, $|p|$. The presence of -functions in the expressions for the distribution functions, $f^{N=D}$ and $\tilde{f}^{N=D}$, cuts off a part of the high momentum region, but this is a minor effect. Effect of "softening" caused by the -functions is also illustrated in Figs. 8 and 9 (dashed lines). These curves are the BS densities in the pole approximation (solid lines) multiplied by $(M_D \quad ! + p_3)$ integrated over cos .

The results presented in Figs. 8 and 9 imply that the relativistic densities appearing in the formulae for the effective distribution functions are enhanced at medium and high momenta. Comparing these results with those in Figs. 2 and 5 we find that the effect is much larger than any model differences. Still, since the effect is concentrated at high momenta it is not clear if it leads to observable effects in deep inelastic scattering. To clarify this, in Fig. 10 we present the effective distribution function, $f^{N=D}(y)$. For completeness of the illustration, we compare distribution functions calculated using three different charge densities: (i) nonrelativistic density of the Bonn potential (dotted line), (ii) relativistic BS density in the one pole approximation (solid curve) and (iii) exact densities within the BS approach (dashed curve). The last curve is aimed to illustrate differences in the description of the mechanism of the reaction in nonrelativistic and relativistic approaches, i.e. it presents result for made up situation, if charge density of the nonrelativistic model is exactly the same as of the BS approach. We find that consistent relativistic description gives the effective distribution which is systematically harder at high momentum fraction, y. This is a result of harder charge density in the one pole approximation. It is interesting that the relativistic distribution is also enhanced at small y ! 0. This effectively corresponds to larger "binding effects" in the BS approach which was observed in ref. [2]. Very similar effects can be observed in other effective distribution functions, $f^{N=D}$ and $f^{N=D}$. However, in these cases those effects are not so explicit, because of the oscillating nature of the distribution functions. (See e.g. discussion about $f^{N=D}$ below.)

IV. NUMERICAL CALCULATION OF STRUCTURE FUNCTIONS

A. Unpolarized deuteron, F_2^D

The spin-independent SF of the deuteron, F_2^D is calculated using the effective distribution functions presented in Fig. 10 (see discussion at the end of the Section IIIF). The results of this calculation are shown in Fig. 11 in the form of ratio of the SF of the deuteron and the nucleon. The nucleon SF, F_2^N is taken from ref. [42] at $Q^2 = 10\ GeV^2$. We find that BS approach gives a behavior of the deuteron SF qualitatively similar to the results of the nonrelativistic and "made up nonrelativistic" calculations. However, there are two delicate, but essential differences:

First, the ratio F_2^D/F_2^N in the BS approach is lower than others at small x, $x < 0.5$. This effect can be easily understood from the form of distribution, $f^{N/D}(y)$, in Fig. 10 and formula (3.23). Indeed, at $x = 0$ the SF F_2^D is:

$$F_2^D(0) = F_2^N(0) \int_0^{M_D/m} f^{N/D}(y)dy: \tag{4.1}$$

Therefore, $F_2^D(0)/F_2^N(0) = 1$ because $\int_0^{M_D/m} f^{N/D}(y)dy = 1$ is a normalization, (3.30). When we move from $x = 0$ to larger x, we "lose" part of the normalization, since the lower limit of integral in eq. (3.23) is x. Since the relativistic $f^{N/D}$ is larger at small x than the nonrelativistic ones, it leads to a faster decrease of the relativistic SF with increasing x. The fact that the ratio F_2^D/F_2^N is less than 1 at small and intermediate x is know to be a result of the "binding of nucleons" (see e.g. [15{17,1] and references therein).

Second, the relativistic SF displays sharper rise at higher x, $x > 0.5$ than the nonrelativistic ones. This, again, can be understood from the form of the distribution, Fig. 10, and the convolution formula, (3.23). With increasing of x the role of the high momentum tail of the effective distribution is getting more important for integration in eq. (3.23) and at $x > 1.0$ the tail is completely dominating. The deuteron SF at $x > 1$ is presented in Fig. 12.

It has been shown recently, that relativistic calculations lead to the larger binding effects than the non-relativistic ones [9,2]. However, the result of ref. [9] which presents effects two to three times larger than ours still is neither explained nor physically understood. In ref. [2] the size of the effect was not so large, but the method of numerical calculations was essentially based on the numerical inverse Mellin transform of the non-analytical function. The approximations had to be made, which eventually was not good at high momentum. That is why we specially attempted to verify quantitative size of the effect. It is worth to remember that we discuss quite tiny effect of $1 \quad 2\%$ in the ratio F_2^D/F_2^N. We also can measure the binding effect using the energy-momentum sum rule (3.29). The quantity $_N$ is a natural parameter controlling the binding in any particular calculations. For example, the nonrelativistic formulae allow for an analytical estimate of $_N$ which essentially gives us an idea about size of the effect [16,17,2]:

$$= \frac{\varepsilon_D}{m} \quad \frac{\langle T \rangle}{6m}; \tag{4.2}$$

where $\langle T \rangle$ is a nonrelativistic mean kinetic energy of nucleons in the deuteron. For the realistic models typically $\langle T \rangle$ 15 MeV, which gives 5 10^{3}. Calculating with the BS effective distribution of the present paper, we find 0:7 10^{3}. Note, that in ref. [2] the quantity 1 10^{3} has been reported. We attribute this small discrepancy to the less sophisticated numerical approximation which had been made in [2]. This approximation slightly underestimates a high momentum behavior of $f^{N=D}$.

B. Polarized deuteron, b_1^D and b_2^D

The SFs of the deuteron $b_{1,2}^D(x)$ are calculated within both the relativistic and nonrelativistic approaches. The relativistic calculations are based on the formulae (3.21), (3.22)–(3.25). The nonrelativistic calculations, eq. (3.40), uses the realistic wave function of the deuteron in the Bonn potential [19]. Another ingredient of the calculations, the nucleon SFs $F_{1,2}^N(x;Q^2)$, is again taken from ref. [42] at $Q^2 = 10\ \mathrm{GeV}^2$. The results are neither very sensitive to the particular choice of the parametrization for the nucleon SFs nor to the Q^2-dependence of them.

The distribution functions $f^{N=D}(y)$ are calculated and the results are presented in Fig. 13. The relativistic (solid line) and nonrelativistic (dotted line) calculations give similar behavior of the distribution function. Indeed, it is difficult to distinguish between them, not speaking about making definite conclusions. The third line in the Fig. 13 is given for illustration, and presents $y\, f^{N=D}(y)$ for the relativistic calculations. The calculation of the sum rules is more representative. To understand the scale of effects, which are discussed below, it is customary to define auxiliary quantities:

$$\int_0^{M_Z/m} \mathrm{Abs}\ f^{N=D}(y)\ dy \simeq \int_0^{M_Z/m} \mathrm{Abs}\ y\, f^{N=D}(y)\ dy \simeq 0{:}14: \tag{4.3}$$

The Bethe-Salpeter and nonrelativistic Bonn calculations give the same result in (4.3), with accuracy of 5%. Thus, the effective distribution functions, $f^{N=D}$, are an order of magnitude smaller than the usual spin-independent distributions $f^{N=D}$ normalized to 1. This is not a very important circumstance, but it works against accuracy in the numerical calculations, since $f^{N=D}$ is a difference of two functions normalized to 1 ($M = 1$ and $M = 0$). Numerically, the sum rule (3.34) (see also eq. (3.41)) is satisfied both in relativistic and nonrelativistic calculations with good accuracy, despite the approximate numerical "inverse Wick rotation" and the discussion after eq. (3.40). The corresponding integrals are 5 10^{4} and 3 10^{5} and they should be compared to the estimate (4.3). The sum rule (3.28) may be used to improve distributions $f^{N=D}$ by making integrals for $f_1^{N=D}$ and $f_0^{N=D}$ exactly the same. However, this does not lead to a significant variation of results for SFs, except $x \to 0$ for $b_1^D(x)$.

The behavior of $b_1^D(x)$ at $x \to 0$ deserves to be considered more closely, especially for numerical calculations, since the nucleon function $F_1^N(x)$ can be divergent at small x. Unfortunately it is impossible to estimate $b_1^D(0)$ exactly for the realistic SF F_1^N. However, a contribution of the singularity can be evaluated. Indeed, let us assume a singular behavior as $F_1^N \quad C/x$, then eq. (3.22) leads for small x to

$$b_1^D(x \to 0) \quad \frac{C}{x}\int_x^{M_Z=m} f^{N=D}(y)dy = \frac{C}{x}\left\{\int_0^{M_Z=m} \int_0^{Zx}\right\} f^{N=D}(y)dy$$

$$\frac{C}{x}\int_x^{Z} C\, f^{N=D}(0); \tag{4.4}$$

where $Z = 0$ in exact relativistic formula, but it can be a small number in numerical calculations or in the nonrelativistic formalism. Thus, the limit of the deuteron SF $b_1^D(x)$ as $x \to 0$ is a constant, but one has to exercise great care in performing numerical computations, since any error leads to a divergent behavior at small x. In this context, an adjustment of norms of the two terms in formulae (3.25) and (3.40) has a meaning of subtraction of the numerical error from b_1^D at small x.

The situation with the second sum rule (3.35) is quite different. Numerically it is violated more significantly than the previous one. Corresponding integrals are $1 \quad 10^3$ and $3 \quad 10^3$ for relativistic and nonrelativistic calculations respectively, i.e. about 0:7% and 2% compare to (4.3). Therefore, numerical approximations slightly damage the relativistic formula too. It is attributed to the numerical rotation in the Minkowski space. An adjustment of the normalization, as it has been discussed, slightly improves the accuracy (to 0:5%). On the contrary, the result for the nonrelativistic approach is stable with respect to any adjustments, since it is defined by the formulae (3.42).

The SFs b_1^D and b_2^D are calculated within two approaches as well. The results are shown in Fig. 14 a) and b). The behavior of the functions in Fig. 14 a) suggests the validity of the sum rule (3.34). At the same time, the nonrelativistic calculation for b_2^D in Fig. 14 b) (dotted line) obviously does not satisfy the sum rule (3.35). The main difference of the relativistic and nonrelativistic calculations is at small x, where these approaches give different signs for the SFs. To illustrate the effect of the presence of the δ-function under integral in the nonrelativistic formula (3.40), the calculations have been done as well with a restricted interval of integration over $|p|$. The condition $|p| < 0{:}7$ GeV corresponds to the \softer" deuteron wave function, but makes the sum rule (3.42) exact. Corresponding SFs are shown in Fig. 14 a) and b) (dashed line). The result of this \experiment" is that the effect of δ-function is not quantitatively significant. It also does not affect the principle conclusion about the second sum rule (3.35), but makes the defect a tiny bit smaller. This is understandable, since the sum rule breaking terms in (3.42) is $\sim |p|\cos$.

C. Polarized deuteron, g_1^D

The spin-dependent SF of the deuteron, g_1^D, is calculated using the same three models as the spin-independent SF, F_2: the fully relativistic BS approach (solid line), nonrelativistic approach based on the Bonn wave function (dotted line) and nonrelativistic approach which uses the exact density of the BS approach (dashed line). The nucleon SF, g_1^N is taken from ref. [43]. The results of calculations are presented in Fig. 15.

For illustration we also present in Fig. 15 the quantity $h_{5\ 3}i^{BS}_{M=1}$ which corresponds to a \model" for the deuteron SF (dot-dashed straight line):

$$g_1^D(x;Q^2) = \frac{1}{4} h_{5\ 3}i^{BS}_{M=1} \quad {}^N_1g(x;Q^2): \tag{4.5}$$

If we replace $h_{5\ 3}i^{BS}_{M=1}$ by the factor $(1 \quad 3{=}2 \quad {}_Dw)$ from eq. (2.18), we get the formula usually used by experimentalists aiming to obtain the neutron SF, g_1^n from the combined proton and deuteron data.

Fig. 15 shows that picture is different from the naive estimate (4.5). However, within the present day experimental errors it may be a reasonable approximation (see e.g. ref. [4]). Huge leaps of the ratio around the constant $h_{5\ 3}i^{BS}_{M=1}$ at $x < 0.7$ are not too important. They correspond to zeros of the nucleon SF which are slightly shifted by the convolution formula. Systematic difference in the ratio exist between the nonrelativistic calculation (dotted line) and two calculations based on the BS densities (solid and dashed curves). This is a difference between D-wave admixture in the Bonn potential (w_D 4.3%) and our solution of the BS equation (w_D 5%). The rise of the ratio, at x higher than 0.7, is of the same nature as in the spin-independent case in Fig. 11, it is caused by the Fermi motion.

V. SUMMARY

In this paper, we have presented a study of the deep inelastic electron scattering on the deuteron in the Bethe-Salpeter formalism in the realistic meson-nucleon model. In particular,

- The connection of the structure functions to the densities of the appropriate charges and currents is analyzed. By analysing the same densities in the nonrelativistic approach, we have systematically compared the relativistic and nonrelativistic calculations, and established sources of the relativistic effects.

- Using our numerical solution of the Bethe-Salpeter equation amplitude with a realistic kernel, the leading twist structure functions of the deuteron, F_2^D, $b_{1,2}^D$ and g_1^D, are calculated in the fully relativistic fashion.

- Our numerical calculations of the structure functions emphasize a qualitative agreement with previous non-relativistic results. However, we have found effects systematically distinguishing a consistent relativistic approach from the nonrelativistic one: in the relativistic formalism (i) the magnitude of binding effects is larger and (ii) the effect of Fermi motion at high x is stronger; and (iii) the nonrelativistic calculations suffer unavoidable internal inconsistencies, which lead to small effects in the structure functions F_2^D and g_1^D, but seriously damage structure function $b_{1,2}^D$ and noticably break sum rules for this function.

The present paper concludes our systematic study of the deep inelastic electron (muon) scattering on the deuteron in the Bethe-Salpeter formalism. The results are collected in the two papers, ref. [1] and the present paper, and in part have been also published previously in refs. [2{4,30]. The main lesson, we have learned from this study, is that the deuteron in the deep inelastic reaction indeed behaves as a very slightly relativistic system. One has to look for special conditions or kinematics of the reaction to be able to find noticible relativistic effects. We have found certain situations where the relativistic approach is absolutely essential and use of the nonrelativistic methods is not justified. Most representative examples are the high x behaviour of the structure funtions and the spin-dependent structure functions, $b_{1,2}^D$.

Apart from the phenomenological differences between the relativistic and nonrelativistic approaches, the most important merit of the covariant formalism is its consistency. Its close connection to the field theory guaranties that the calculated observables obey the sum rules and other general properties imposed by the

fundamental principles. In this sense the relativistic approach is definitely more advanced theoretically than its nonrelativistic counterpart and provides a better understanding of the deep inelastic scattering on the deuteron.

ACKNOWLEDGMENTS

We would like to thank F. Gross, W. Van Orden and J. Tjon for conversations about properties of the relativistic equations and its solutions. Authors also wish to thank everybody who had discussed various topics of this paper with us. In particular, we would like to thank S. Bondarenko, V. Burov, C. Ciodegli Atti, S. Dorkin, A. Efremov, B. Kampfer, K. Kazakov, S. Kulagin, W. Melnitchouk, A. Molochkov, S. Scopetta, C. Shakin, S. Simula, O. Teryaev, A. Titov, A. Thomas and W. Weise.

The research was supported in part by the Natural Sciences and Engineering Research Council of Canada and by Instituto Nazionale di Fisica Nucleare, Sezione di Perugia, Italy.

APPENDIX A: EXPLICIT FORMULAE FOR DENSITIES

In this Appendix we present formulae which allow to restore explicit form of the various densities in the BS formalism. For convenience, we define auxiliary \densities":

$$\begin{pmatrix} f_0^{N=D}(p) \\ f_3^{N=D}(p) \end{pmatrix} = \frac{1}{3}\sum_M \int_0^{Z^2} d\,\mathrm{Tr}\,\Big[\,{}_M(p_0;p)\begin{pmatrix} 0 \\ 3 \end{pmatrix}{}_M(p_0;p)(\hat{p}_2 - m)\Big]; \tag{A1}$$

$$\begin{pmatrix} f_0^{N=D}(p) \\ f_3^{N=D}(p) \end{pmatrix} = \int_0^{Z^2} d\,\mathrm{Tr}\,\Big[\,{}_M(p_0;p)\begin{pmatrix} 0 \\ 3 \end{pmatrix}{}_M(p_0;p)(\hat{p}_2 - m)\Big]_{M=1} \int_0^{Z^2} d\,\mathrm{Tr}\,f::g_{M=0}; \tag{A2}$$

$$\begin{pmatrix} f_0^{N=D}(p) \\ f_3^{N=D}(p) \end{pmatrix} = \int_0^{Z^2} d\,\mathrm{Tr}\,\Big[\,{}_M(p_0;p)\begin{pmatrix} 5 & 0 \\ 5 & 3 \end{pmatrix}{}_M(p_0;p)(\hat{p}_2 - m)\Big]_{M=1}; \tag{A3}$$

where integration over leads to the trivial factor of 2, since none of the matrix elements on the r.h.s. depends on . To obtain explicit expressions for the densities discussed in the paper we have to compare eq. (A1)–(A3) with definitions of corresponding densities.

Note, that a formalism presented in refs. [1,2] and in this paper can be easily adopted for an analytical computer calculations. The following results have been obtained utilizing the Mathematica package [44]:

$$\begin{aligned} f_0^{N=D}(p) = {} & m\,\big(8\,{}_{a0}(p_0;p)\,{}_{t0}(p_0;p) - 8\,{}_{a2}(p_0;p)\,{}_{t2}(p_0;p)\big) \\ & + p\,\Big[\frac{8\,{}_{p1}(p_0;p)\,{}_{t0}(p_0;p)}{p\sqrt{3}} + 8\sqrt{\frac{2}{3}}\,{}_{p1}(p_0;p)\,{}_{t2}(p_0;p) \\ & + 4\sqrt{\frac{2}{3}}\,{}_{a0}(p_0;p)\,{}_{v1}(p_0;p) + \frac{4\,{}_{a2}(p_0;p)\,{}_{v1}(p_0;p)}{p\sqrt{3}}\Big] \\ & + \tfrac{1}{2}M\,d\,p_0\,\big[2\,{}^0_{a1}(p_0;p)^2 + 2\,{}_{a0}(p_0;p)^2 + 2\,{}_{a2}(p_0;p)^2 + 2\,{}_{p1}(p_0;p)^2 \\ & + 8\,{}_{t0}(p_0;p)^2 + 8\,{}_{t2}(p_0;p)^2 + 8\,{}^0_{t1}(p_0;p)^2 + 2\,{}_{v1}(p_0;p)^2 \end{aligned} \tag{A4}$$

$$f_3^{N=D}(p) = \cos(\ ) \tag{A 5}$$

$$\begin{aligned}
&\tfrac{1}{2}M_d \quad p_0 \quad \frac{8\ {}_{p1}(p_0;p)\ {}_{t0}(p_0;p)}{\sqrt{3}} \quad 8\sqrt{\frac{2}{3}}\ {}_{p1}(p_0;p)\ {}_{t2}(p_0;p) \\
&\qquad 4\sqrt{\frac{2}{3}}\ {}_{a0}(p_0;p)\ {}_{v1}(p_0;p) \quad \frac{4\ {}_{a2}(p_0;p)\ {}_{v1}(p_0;p)}{\sqrt{3}}\Bigg) \\
+ \quad & m \quad \frac{4\ {}_{a0}(p_0;p)\ {}_{p1}(p_0;p)}{\sqrt{3}} + 4\sqrt{\frac{2}{3}}\ {}_{a2}(p_0;p)\ {}_{p1}(p_0;p) \\
&\qquad + 8\sqrt{\frac{2}{3}}\ {}_{t0}(p_0;p)\ {}_{v1}(p_0;p) + \frac{8\ {}_{t2}(p_0;p)\ {}_{v1}(p_0;p)}{\sqrt{3}}\Bigg) \\
+ \quad & p \quad 2\ {}^{0}_{a1}(p_0;p)^2 \quad \frac{2\ {}_{a0}(p_0;p)^2}{3} \quad \frac{8\sqrt{2}\ {}_{a0}(p_0;p)\ {}_{a2}(p_0;p)}{3} \\
&\qquad + \frac{2\ {}_{a2}(p_0;p)^2}{3} \quad 2\ {}_{p1}(p_0;p)^2 + \frac{8\ {}_{t0}(p_0;p)^2}{3} \quad 2\ {}_{v1}(p_0;p)^2 \\
&\qquad + \frac{32\sqrt{2}\ {}_{t0}(p_0;p)\ {}_{t2}(p_0;p)}{3} \quad \frac{8\ {}_{t2}(p_0;p)^2}{3} + 8\ {}^{0}_{t1}(p_0;p)^2\Bigg)
\end{aligned}$$

$$f_0^{N=D}(p) = \cos(\ ) \tag{A 6}$$

$$\begin{aligned}
&\tfrac{1}{2}M_d \quad p_0 \quad 2\sqrt{6}\ {}_{a0}(p_0;p)\ {}_{v1}(p_0;p) + 2\sqrt{3}\ {}_{a2}(p_0;p)\ {}_{v1}(p_0;p) \\
+ \quad & m \quad 4\sqrt{6}\ {}_{t0}(p_0;p)\ {}_{v1}(p_0;p) \quad 4\sqrt{3}\ {}_{t2}(p_0;p)\ {}_{v1}(p_0;p) \\
+ \quad & p \quad 2\ {}_{a0}(p_0;p)^2 + 2\sqrt{2}\ {}_{a0}(p_0;p)\ {}_{a2}(p_0;p) + \ {}_{a2}(p_0;p)^2 \\
&\qquad 8\ {}_{t0}(p_0;p)^2 \quad 8\sqrt{2}\ {}_{t0}(p_0;p)\ {}_{t2}(p_0;p) \quad 4\ {}_{t2}(p_0;p)^2 \\
&\qquad 12\ {}^{0}_{t1}(p_0;p)^2 + 3\ {}_{v1}(p_0;p)^2
\end{aligned}$$

$$f_3^{N=D}(p) = P_2(\cos(\ )) \tag{A 7}$$

$$\begin{aligned}
&p \quad \frac{8\ {}_{p1}(p_0;p)\ {}_{t0}(p_0;p)}{\sqrt{3}} \quad 4\sqrt{\frac{2}{3}}\ {}_{p1}(p_0;p)\ {}_{t2}(p_0;p) \\
&\qquad 2\sqrt{\frac{2}{3}}\ {}_{a0}(p_0;p)\ {}_{v1}(p_0;p) \quad \frac{8\ {}_{a2}(p_0;p)\ {}_{v1}(p_0;p)}{\sqrt{3}}\Bigg) \\
+ \quad & m \quad 4\sqrt{2}\ {}_{a2}(p_0;p)\ {}_{t0}(p_0;p) + 4\sqrt{2}\ {}_{a0}(p_0;p)\ {}_{t2}(p_0;p) \\
&\qquad + 8\ {}_{a2}(p_0;p)\ {}_{t2}(p_0;p) + 4\sqrt{2}\ {}^{0}_{a1}(p_0;p)\ {}^{0}_{t1}(p_0;p) \\
&\qquad 2\sqrt{2}\ {}_{p1}(p_0;p)\ {}_{v1}(p_0;p) \\
+ \quad & \tfrac{1}{2}M_d \quad p_0 \quad 2\sqrt{2}\ {}_{a0}(p_0;p)\ {}_{a2}(p_0;p) \quad 2\ {}_{a2}(p_0;p)^2
\end{aligned}$$

$$8\sqrt{2}\ {}_{t0}(p_0;p)\ {}_{t2}(p_0;p) \quad 8\ {}_{t2}(p_0;p)^2$$

$$8\ {}^{0}_{t1}(p_0;p)^2 \quad 2\ {}_{v1}(p_0;p)^2$$

$$+ \quad p \quad \frac{8\ {}_{p1}(p_0;p)\ {}_{t0}(p_0;p)}{\sqrt{3}} + 4\sqrt{\frac{2}{3}}\ {}_{p1}(p_0;p)\ {}_{t2}(p_0;p)$$

$$4\sqrt{\frac{2}{3}}\ {}_{a0}(p_0;p)\ {}_{v1}(p_0;p) + \frac{2\ {}_{a2}(p_0;p)\ {}_{v1}(p_0;p)}{\sqrt{3}}\ !$$

$$+ \quad m \quad (8\ {}_{a0}(p_0;p)\ {}_{t0}(p_0;p) \quad 4\ {}_{a2}(p_0;p)\ {}_{t2}(p_0;p)$$

$$4\sqrt{2}\ {}^{0}_{a1}(p_0;p)\ {}^{0}_{t1}(p_0;p) + 2\sqrt{2}\ {}_{p1}(p_0;p)\ {}_{v1}(p_0;p)$$

$$+ \ \tfrac{1}{2}M_d \quad p_0 \quad 2\ {}_{a0}(p_0;p)^2 + \ {}_{a2}(p_0;p)^2 \quad 8\ {}_{t0}(p_0;p)^2$$

$$+ 4\ {}_{t2}(p_0;p)^2 \quad 4\ {}^{0}_{t1}(p_0;p)^2 \quad {}_{v1}(p_0;p)^2$$

$$f_0^{N=D}(p) = \quad P_2(\cos(\ )) \tag{A 8}$$

$$m \quad 12\sqrt{2}\ {}_{a2}(p_0;p)\ {}_{t0}(p_0;p) \quad 12\sqrt{2}\ {}_{a0}(p_0;p)\ {}_{t2}(p_0;p)$$

$$+ 12\ {}_{a2}(p_0;p)\ {}_{t2}(p_0;p)$$

$$+ \quad p \quad 8\sqrt{3}\ {}_{p1}(p_0;p)\ {}_{t0}(p_0;p) \quad 8\sqrt{6}\ {}_{p1}(p_0;p)\ {}_{t2}(p_0;p)$$

$$+ 2\sqrt{6}\ {}_{a0}(p_0;p)\ {}_{v1}(p_0;p) + 2\sqrt{3}\ {}_{a2}(p_0;p)\ {}_{v1}(p_0;p)$$

$$+ \ \tfrac{1}{2}M_d \quad p_0 \quad 6\ {}^{0}_{a1}(p_0;p)^2 + 6\sqrt{2}\ {}_{a0}(p_0;p)\ {}_{a2}(p_0;p) \quad 3\ {}_{a2}(p_0;p)^2$$

$$6\ {}_{p1}(p_0;p)^2 + 24\sqrt{2}\ {}_{t0}(p_0;p)\ {}_{t2}(p_0;p) \quad 12\ {}_{t2}(p_0;p)^2$$

$$+ 12\ {}^{0}_{t1}(p_0;p)^2 + 3\ {}_{v1}(p_0;p)^2$$

$$f_3^{N=D}(p) = \quad \cos(\ ) \tag{A 9}$$

$$p \quad 4\ {}_{a0}(p_0;p)^2 + 2\sqrt{2}\ {}_{a0}(p_0;p)\ {}_{a2}(p_0;p) + 4\ {}_{a2}(p_0;p)^2$$

$$+ 16\ {}_{t0}(p_0;p)^2 \quad 8\sqrt{2}\ {}_{t0}(p_0;p)\ {}_{t2}(p_0;p) \quad 16\ {}_{t2}(p_0;p)^2$$

$$+ \ \tfrac{1}{2}M_d \quad p_0 \quad 8\sqrt{3}\ {}_{p1}(p_0;p)\ {}_{t0}(p_0;p) \quad 4\sqrt{6}\ {}_{p1}(p_0;p)\ {}_{t2}(p_0;p)$$

$$2\sqrt{6}\ {}_{a0}(p_0;p)\ {}_{v1}(p_0;p) + 4\sqrt{3}\ {}_{a2}(p_0;p)\ {}_{v1}(p_0;p)$$

$$+ \quad m \quad 4\sqrt{3}\ {}_{a0}(p_0;p)\ {}_{p1}(p_0;p) + 2\sqrt{6}\ {}_{a2}(p_0;p)\ {}_{p1}(p_0;p)$$

$$+ 4\sqrt{6}\ {}_{t0}(p_0;p)\ {}_{v1}(p_0;p) \quad 8\sqrt{3}\ {}_{t2}(p_0;p)\ {}_{v1}(p_0;p)$$

$$+ P_2(\cos(\ ))$$

$$+ \tfrac{1}{2} M_d \quad p_0 \quad 12\sqrt{6}\ {}_{p1}(p_0;p)\ {}_{t2}(p_0;p) \quad 6\sqrt{3}\ {}_{a2}(p_0;p)\ {}_{v1}(p_0;p)$$

$$+ \quad m \quad 6\sqrt{6}\ {}_{a2}(p_0;p)\ {}_{p1}(p_0;p) + 12\sqrt{3}\ {}_{t2}(p_0;p)\ {}_{v1}(p_0;p)$$

$$+ \quad p \quad 6\ {}^{0}_{a1}(p_0;p)^2 \quad 9\ {}_{a2}(p_0;p)^2 + 6\ {}_{p1}(p_0;p)^2$$

$$+ 36\ {}_{t2}(p_0;p)^2 + 12\ {}^{0}_{t1}(p_0;p)^2 \quad 3\ {}_{v1}(p_0;p)^2$$

APPENDIX B: HADRONIC TENSOR FOR THE DEUTERON. PROJECTORS.

The parametrization of hadron tensor for the deuteron, utilized in the present paper, is given by eq. (3.1). It has both symmetric, $\{\ldots\}$, and antisymmetric $[\ldots]$ parts in respect to the permutation of its indices:

$$W^{D} = W^{D}_{\{\ \ \}} + W^{D}_{[\ \ ]}: \tag{B1}$$

Three physical vectors are used in this parametrization:

1. P_D the deuteron momentum. In the rest frame of the deuteron $P_D = (M_D;0)$;
2. q the momentum transfer in the deep inelastic scattering. With proper choice of the orientation of the coordinate system $q = (\ ;0;0;\sqrt{\ ^2 + Q^2})$. In the deep inelastic limit, when $Q^2/\ ^2 \ \ 0$, $pq = \ (p_0 + p_3)$.
3. $S_D(M)$ is the total angular momentum of the deuteron, i.e. spin of the deuteron as an elementary particle:

$$S_D(M) = \frac{i}{M_D} \quad E\ (M)E\ (M)P_D\ ; \tag{B2}$$

$$E(M) = \begin{cases} \frac{1}{\sqrt{2}}(0;\ 1;\ i;0); & M = 1 \\ (0;0;0;1); & M = 0 \\ \frac{1}{\sqrt{2}}(0;1;\ i;0); & M = \ 1 \end{cases} \tag{B3}$$

The symmetric part of the hadron tensor, $W^{D}_{\{\ \ \}}$, contains terms proportional to the two following tensor structures:

$$T^{(1)} = \ g\ + \frac{q\ q}{q^2}; \tag{B4}$$

$$T^{(2)} = \ P_D \quad q\frac{P_D q}{q^2} \quad P_D \quad q\frac{P_D q}{q^2} \quad \frac{1}{P_D q}: \tag{B5}$$

Because of the conservation of the electromagnetic current, the contraction of the hadron tensor with q in respect of any index is zero. That is why only $P_D\ P_D$ and g are available to construct the projection operators to extract structure functions F^D_1 and F^D_2 from the hadron tensor. We introduce the following coefficients:

$$C_1 \quad g \quad T^{(1)}; \quad C_2 \quad g \quad T^{(2)}; \quad C_3 \quad \frac{P_D P_D}{P_D^2} T^{(1)}; \quad C_4 \quad \frac{P_D P_D}{P_D^2} T^{(2)}; \tag{B6}$$

$$D_C \quad C_1 \quad \not{C} \quad C_2 \quad \not{C}; \tag{B7}$$

$$A_1 \quad g \quad W^{D}; \quad A_2 \quad \frac{P_D P_D}{P_D^2} W^{D}: \tag{B8}$$

Then the structure function are recovered by:

$$F_1^D = \frac{A_1 \quad \not{C} \quad A_2 \quad \not{C}}{D_C}; \tag{B9}$$

$$F_2^D = \frac{A_2 \quad \not{C} \quad A_1 \quad \not{C}}{D_C}: \tag{B10}$$

The antisymmetric part of the hadron tensor of the deuteron, $W^{D}_{[\ \ ]}$, in the general case has a form:

$$W^{D}_{[\ \ ]} = \frac{iM_D}{P_D q} \quad q \quad S_D (M) \; g_1^D (x_D; Q^2) + g_2^D (x_D; Q^2) \quad P_D \frac{(S_D (M) q)}{P_D q} g_2^D (x_D; Q^2) \quad ; \tag{B11}$$

where the second structure function, g_2^D, is vanishing in the deep inelastic limit, $\quad ! \quad 1$; $Q^2 \; ! \; 1$; $Q^2 = \quad ! \quad$ const. We do not discuss this structure function in the present paper. To obtain the spin-dependent structure function, g_1^D, we construct the antisymmetric projectors. The two following projectors are equivalent for our purpose:

$$R^{(1)} \quad i \quad q \; S_D (M); \tag{B12}$$

$$R^{(2)} \quad \frac{i(S_D (M) q)}{P_D q} \quad q \; P_D: \tag{B13}$$

It is interesting that in the limit $Q^2 = {}^2 \; ! \; 0$:

$$g_1^D = \frac{R^{(1)} \quad W^{D}}{2} = \frac{R^{(2)} \quad W^{D}}{2}: \tag{B14}$$

---

[1] A.Yu. Umnikov and F.C. Khanna, Phys. Rev. C 49, 2311 (1994); Mod. Phys. Lett. A 10, 91 (1995).

[2] A.Yu. Umnikov, L.P. Kaptari, K.Yu. Kazakov and F. Khanna, Phys. Lett. B 334, 163 (1994).

[3] F.C. Khanna, L.P. Kaptari and A.Yu. Umnikov, Czech. J. Physics, 45, 363 (1995). (Lectures at the Indian-Summer School on Electron Scattering of Nucleons and Nuclei, Prague (Czech Republic), September 1994.)

[4] A.Yu. Umnikov, L.P. Kaptari, K.Yu. Kazakov and F.C. Khanna, AIP Conference Proceedings 334, ed. F. Gross (AIP, 1995) 749–752. (Proc. 14-th Int. Conference on Few Body Problem in Physics, Williamsburg, Virginia, 1994);
AIP Conference Proceedings 339, eds. E.J. Stephenson and S.E. Vigdor (AIP, 1995) 79–86. (Proc. 11-th Int. Simposium on High Energy Spin Physics and 8-th Int. Simposium on Polarization Phenomena in Nuclear Physics, Bloomington, Indiana, 1994.)

[5] W. Melnitchouk, A.W. Schreiber and A.W. Thomas, Phys. Rev. D 49, 1183 (1994).

[6] W. Melnitchouk, A.W. Schreiber and A.W. Thomas, Phys. Let. B 335, 11 (1995).

[7] W. Melnitchouk, G. Piller and A.W. Thomas, Phys. Let. B 346, 165 (1995).

[8] S. Kulagin, W. Melnitchouk, G. Piller and W. Weise, Phys. Rev. C 52, 932 (1995).

[9] M. Braun and M. Tokarev, Phys. Lett. B 320, 381 (1994).

[10] F. Lev, e-print archive: hep-ph/9501348; hep-ph/9507421.

[11] L.I. Frankfurt and M.S. Strikman, Phys. Lett. B 64, 433 (1976); ibid. B 65, 51 (1976); ibid B 76, 333 (1978).

[12] P.V. Landsho and J.C. Polkinghorne, Phys. Rev. D 18, 153 (1978).

[13] D. Kusno and M.J. Moravcsik, Phys. Rev. D 20, 2734 (1979).

[14] P.J. Mulders, A.W. Schreiber and H. Meyer, Nucl. Phys. A 549, 498 (1992).

[15] S.V. Akulinichev, S.A. Kulagin, G.M. Vagradov, Phys. Lett. 158B, 485 (1985); Jetp Lett. 42, 127 (1985).

[16] B.L. Birbrair, E.M. Levin and A.G. Shuvaev, Nucl. Phys. A 496, 704 (1989).

[17] L.P. Kaptari, A.Yu. Umnikov and B. Kampfer, Phys. Rev. D 47, 3804 (1993).

[18] M. Lacombe, B. Loiseau, J.M. Richard, R. Vinh Mau, J. Côte, P. Pires and R. de Tourreil, Phys. Rev. C 21, 861 (1980).

[19] R. Machleid, K. Holinde and Ch. Elster, Phys. Rep. 149, 1 (1987).

[20] W.W. Buck and F. Gross, Phys. Rev. C 20, 2361 (1979).

[21] M.J. Zuilhof and J.A. Tjon, Phys. Rev. C 22, 2369 (1980).

[22] F. Gross, J.W. Van Orden and K. Holinde, Phys. Rev. C 45, 2094 (1992).

[23] See, e.g. the following papers and references therein:
M.C. Birse and B. Krippa, Phys. Lett. B 373, 9 (1996).
H. Shiomi and T. Hatsuda, Nucl. Phys. A 594, 294 (1995).

[24] See, e.g. the following papers and references therein:
C.A. da Rocha and M.R. Robilotta, Phys. Rev. C 52, 531 (1995); ibid. C 49, 1818 (1994).
C. Ordonez, L. Ray and U. van Kolck, Phys. Rev. C 53, 2086 (1996).

[25] J. Fleischer and J.A. Tjon, Nucl. Phys. B 84, 375 (1975); Phys. Rev. D 15, 2537 (1977).

[26] F. Gross, Proc. 9th Amsterdam miniconference February 1-2, 1996, "Electromagnetic studies of the deuteron", NIKHEF, Amsterdam, 1996, p. 1.

[27] R.A. Arndt, I.I. Strakovskii and R.L. Workman, Phys. Rev. C 50, 2731 (1994).

[28] A.Yu. Umnikov and F.C. Khanna, Int. J. Mod. Phys. A 10, 3935 (1996).

[29] A. Umnikov, Parametrization of Realistic Bethe-Salpeter Amplitude for the Deuteron, e-print archives hep-ph/9605292.

[30] L.P. Kaptari, A.Yu. Umnikov, S. Bondarenko, K. Kazakov, F.C. Khanna and B. Kampfer, to appear in Phys. Rev. C; e-print archive: nucl-th/9603022.

[31] K.G. Wilson, Phys. Rev. 179, 1499 (1969); R.A. Brandt and G. Preparata, Nucl. Phys. B 27, 541 (1971); W. Zimmermann, Ann. Phys. (N.Y.) 77, 570 (1973).

[32] C. Cio degli Atti, L.P. Kaptari, K. Yu. Kazakov, S. Scopetta and A.Yu. Umnikov, Phys. Rev. C 51, 52 (1995).

[33] F. Gross and S. Liuti, Phys. Rev. C 45, 1374 (1992).

[34] A.V. Efremov and O.V. Teryaev, Sov. J. Nucl. Phys. 36, 557 (1982).

[35] L.I. Frankfurt and M.S. Strickman, Phys. Rep. 76, 216 (1981); Nucl. Phys. A 405, 557 (1983).

[36] R.L. Jaffe and A. Manohar, Nucl. Phys. B 321, 343 (1989).
P. Hoodbhoy, R.L. Jaffe and A. Manohar, Nucl. Phys. B 312, 571 (1989).

[37] L.P. Kaptari and A.Yu. Umnikov, Z. Phys. A 341, 353 (1992).

[38] R.L. Jaffe, in: Relativistic dynamics and quark-nuclear physics, eds. M.B. Johnson and A. Picklesimer (Wiley, New York, 1987) 537.

[39] A.Yu. Umnikov, L.P. Kaptari, and F. Khanna, Phys. Rev. C 53, 377 (1996).

[40] S. Kulagin, Nucl. Phys. A 500, 653 (1989).

[41] L.S. Celenza, C.M. Shakin and W. Koepf, Phys. Rev. C 42, 1989 (1990).

[42] L.P. Kaptari and A.Yu. Umnikov, Phys. Lett. B 259, 155 (1991).

[43] A. Schafer, Phys. Lett. B 208, 175 (1988).

[44] S. Wolfram, Mathematica, Addison-Wesley (Reading, Massachusetts, 1993).

meson B	coupling constants $g_B^2=(4\ \ )$; $[g_v=g_t]$	mass $_B$, GeV	cut-o ,GeV	isospin
	12.2	0.571	1.29	0
	1.6	0.961	1.29	1
	14.5	0.139	1.29	1
	4.5	0.549	1.29	0
!	27.0; [0]	0.783	1.29	0
	1.0; [6]	0.764	1.29	1
m = 0:939 GeV, $"_D$ = 2:225 MeV				

Table 1. The set of parameters of the kernel of BS equation used in this work.

FIG. 1. Triangle graph for nucleon contribution to the deuteron matrix element of operator $\hat{O}$.

FIG. 2. The charge density in the deuteron, eqs. (2.9) and (2.11) calculated in different models, nonrelativistic and relativistic. Curves: the Bethe-Salpeter amplitude (solid), the Bonn wave function (dashed), the Paris wave function (dotted).

FIG. 3. The $\langle \tau_3 \rangle(p)$ in the deuteron calculated in different models. Curves: BS amplitude (solid), the Bonn wave function (dashed), the Paris wave function (dotted).

FIG. 4. The "tensor density" of the deuteron, $\langle \tau_0 \rangle^{NR}_{M=1}(p) - \langle \tau_0 \rangle^{NR}_{M=0}(p)$, calculated in different models. To exclude the angular dependence the densities are divided by $P_2(\cos\theta)$. Curves: BS amplitude (solid), the Bonn wave function (dashed), the Paris wave function (dotted).

FIG. 5. The spin density, $\langle \sigma_5 \tau_3 \rangle_{M=1}(p)$, in the deuteron calculated in different models (see Section IIB for definitions). To exclude the angular dependence for the present figure, densities are integrated over all angles. Curves: BS amplitude (solid), the Bonn wave function (dashed), the Paris wave function (dotted).

FIG. 6. The one-pole contribution to the charge density of the deuteron, $\langle \tau_0 \rangle^{BS}_{pole}(p)$, calculated with the BS amplitude. Curves: the leading term in the Taylor expansion (dotted), first two terms, up to $\sim p_2^2$ (dashed), first three terms, up to $\sim p_4^2$ (solid).

FIG. 7. The one-pole contribution to the spin density, of the deuteron, $\langle \sigma_5 \tau_3 \rangle^{BS}_{pole}(p)$, calculated with the BS amplitude. Curves: the leading term in the Taylor expansion (dotted), first two terms, up to $\sim p_2^2$ (dashed), first three terms, up to $\sim p_4^2$ (solid).

FIG. 8. Different "versions" of the charge density of the deuteron calculated with the BS amplitude. Curves: exact, $\langle \tau_0 \rangle^{BS}(p)$ (dotted); in the pole approximations, $\langle \tau_0 \rangle^{BS}_{pole}(p)$, (solid). Dashed curve presents effective density for deep inelastic scattering which is the density in the pole approximation with account for the θ-function cut-off at high momenta.

FIG. 9. The same as in Fig. 8, but for the spin-density, $\langle \sigma_5 \tau_3 \rangle^{BS}(p)$.

FIG. 10. The effective distribution for the nucleon contribution in the deuteron structure function F_2^D, $f^{N=D}(y)$. Curves: fully relativistic BS (solid); nonrelativistic Bonn (dotted), nonrelativistic, but using the BS charge density (dashed).

FIG. 11. The ratio of the deuteron and nucleon structure functions, F_2^D/F_2^N, calculated in different models. Curves correspond to three effective distributions from Fig. 10: fully relativistic BS (solid); nonrelativistic Bonn (dotted), nonrelativistic, but using the BS charge density (dashed).

FIG. 12. The deuteron structure function $F_2^D(x)$ at large x, calculated in different models. Curves correspond to three effective distributions from Fig. 10: fully relativistic BS (solid); nonrelativistic Bonn (dotted), nonrelativistic, but using the BS charge density (dashed). Dash-dotted curve present the free nucleon structure function, F_2^N.

FIG. 13. The effective distribution functions for the deuteron structure functions, $b_{1,2}^D$, $f^{N/D}(y)$, calculated in different models. Curves: fully relativistic BS (solid); nonrelativistic Bonn (dotted). The dashed curve presents $y\,f^{N/D}(y)$.

FIG. 14. The deuteron structure functions b_1^D (a) and b_2^D (b), calculated in different models. Curves: fully relativistic BS (solid); nonrelativistic Bonn (dashed). The dotted curve presents $b_{1,2}^D$ calculated with the "soft" nucleon distribution, the Bonn distribution but cut-off at $|p| > 0.7$ GeV.

FIG. 15. The ratio of the deuteron and nucleon spin-dependent structure functions, g_1^D/g_1^N, calculated in different models. Curves correspond to three effective distributions: fully relativistic BS (solid); nonrelativistic Bonn (dotted), nonrelativistic, but using the BS spin density (dashed).

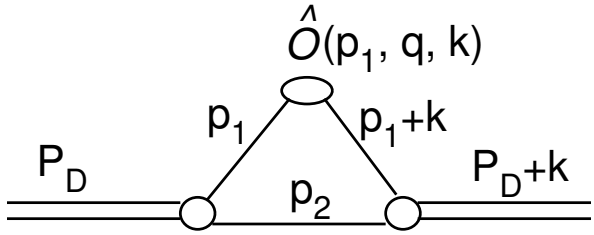
$\hat{O}(p_1, q, k)$
p_1
p_1+k
P_D
P_D+k
p_2

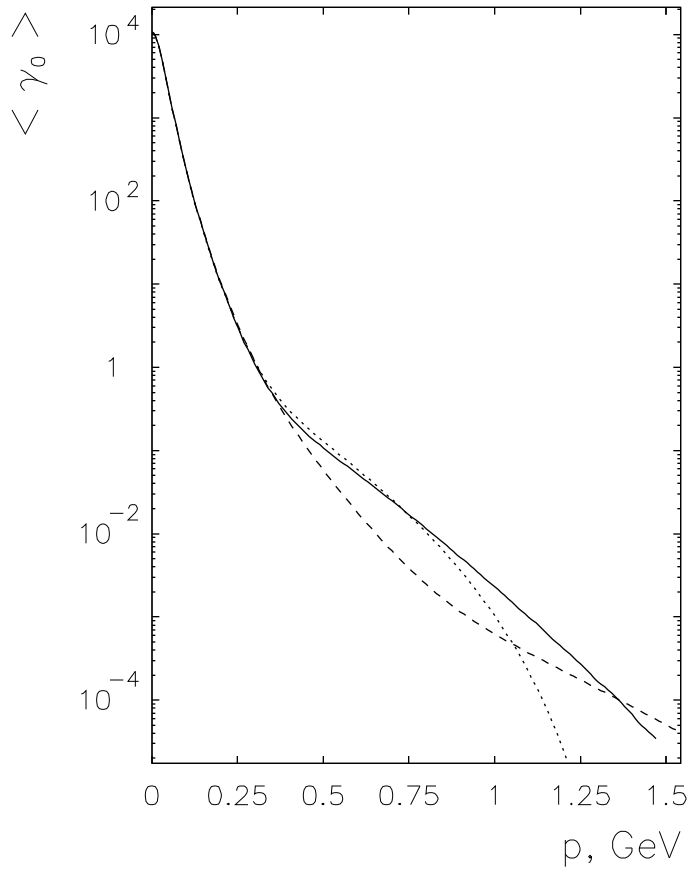
$< \gamma_0 >$
10^4
10^2
1
10^{-2}
10^{-4}
0
0.25
0.5
0.75
1
1.25
1.5
p, GeV

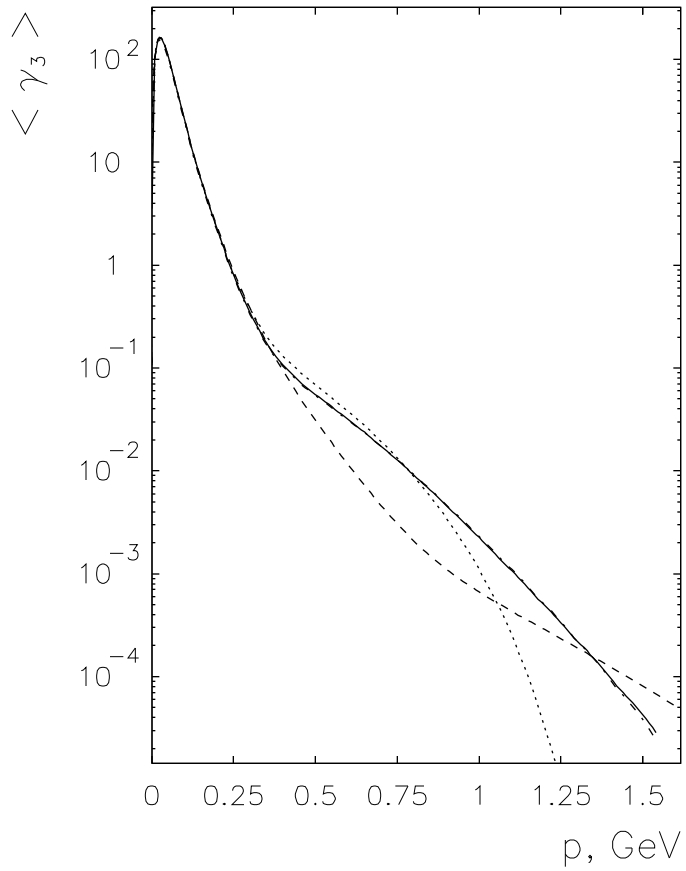
$< \gamma_3 >$
10^2
10
1
10^{-1}
10^{-2}
10^{-3}
10^{-4}
0
0.25
0.5
0.75
1
1.25
1.5
p, GeV

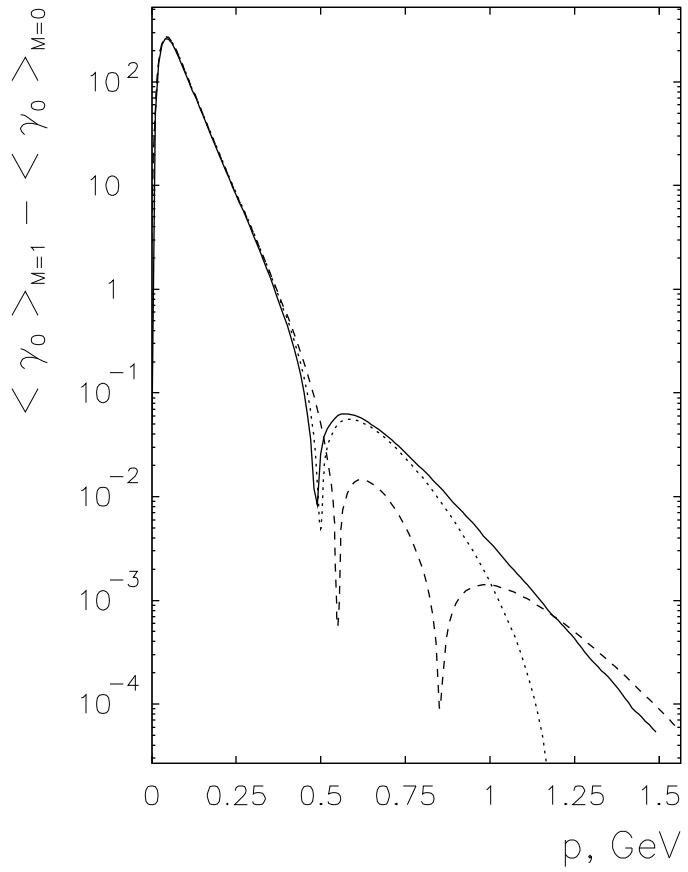
$< \gamma_0 >_{M=1} - < \gamma_0 >_{M=0}$
10^2
10
1
10^{-1}
10^{-2}
10^{-3}
10^{-4}
0
0.25
0.5
0.75
1
1.25
1.5
p, GeV

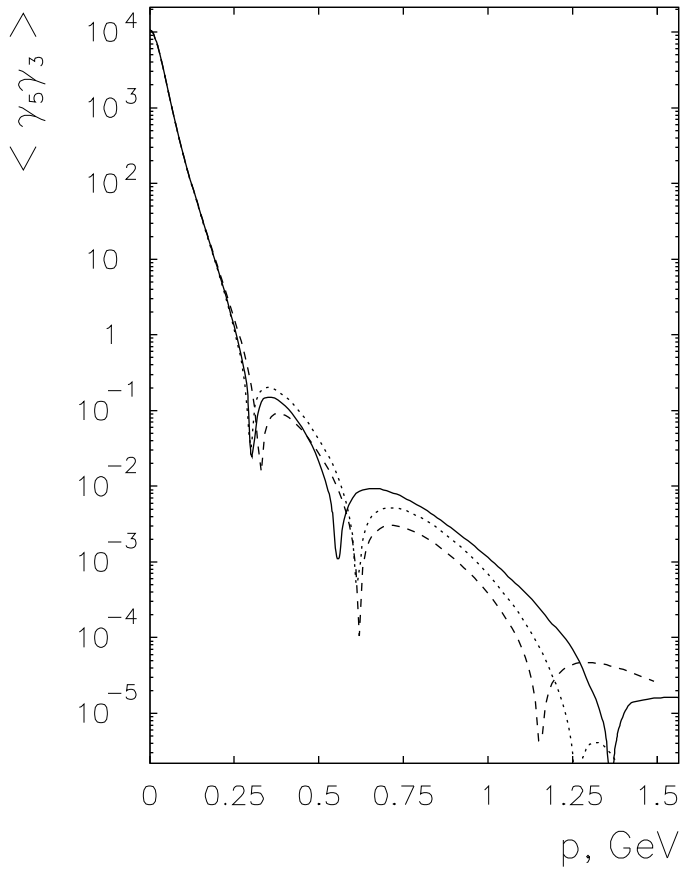
$< \gamma_5 \gamma_3 >$
10^4
10^3
10^2
10
1
10^{-1}
10^{-2}
10^{-3}
10^{-4}
10^{-5}
0
0.25
0.5
0.75
1
1.25
1.5
p, GeV

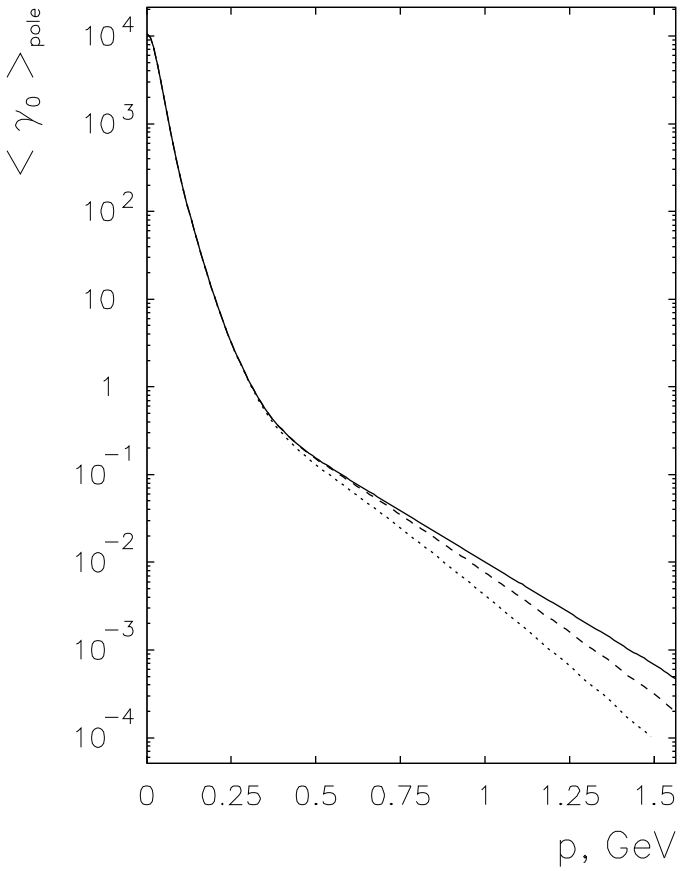
$< \gamma_0 >_{pole}$
10^4
10^3
10^2
10
1
10^{-1}
10^{-2}
10^{-3}
10^{-4}
0
0.25
0.5
0.75
1
1.25
1.5
p, GeV

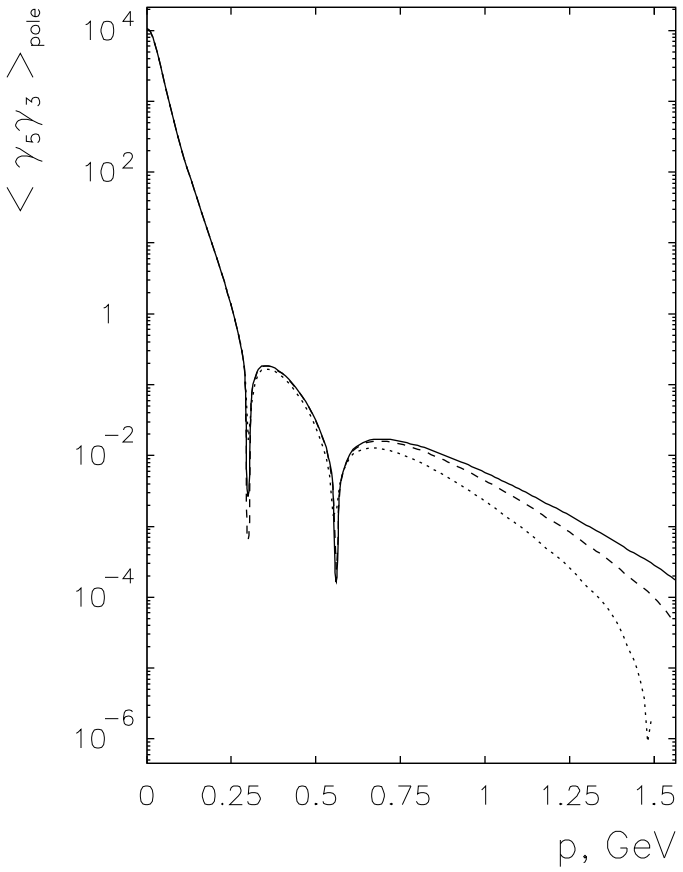
$< \gamma_5 \gamma_3 >_{pole}$
10^4
10^2
1
10^{-2}
10^{-4}
10^{-6}
0
0.25
0.5
0.75
1
1.25
1.5
p, GeV

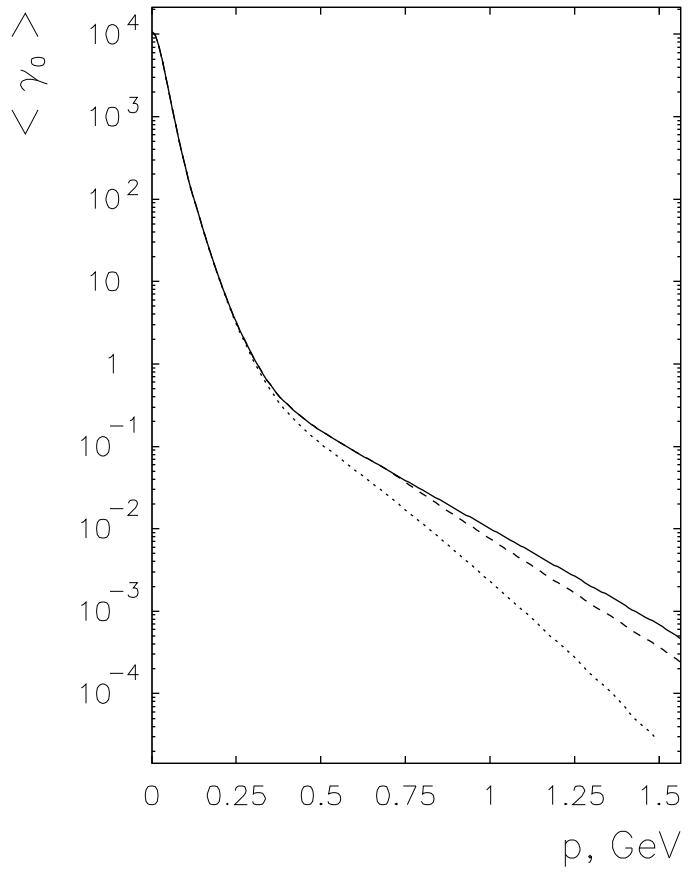
$< \gamma_0 >$
10^4
10^3
10^2
10
1
10^{-1}
10^{-2}
10^{-3}
10^{-4}
0
0.25
0.5
0.75
1
1.25
1.5
p, GeV

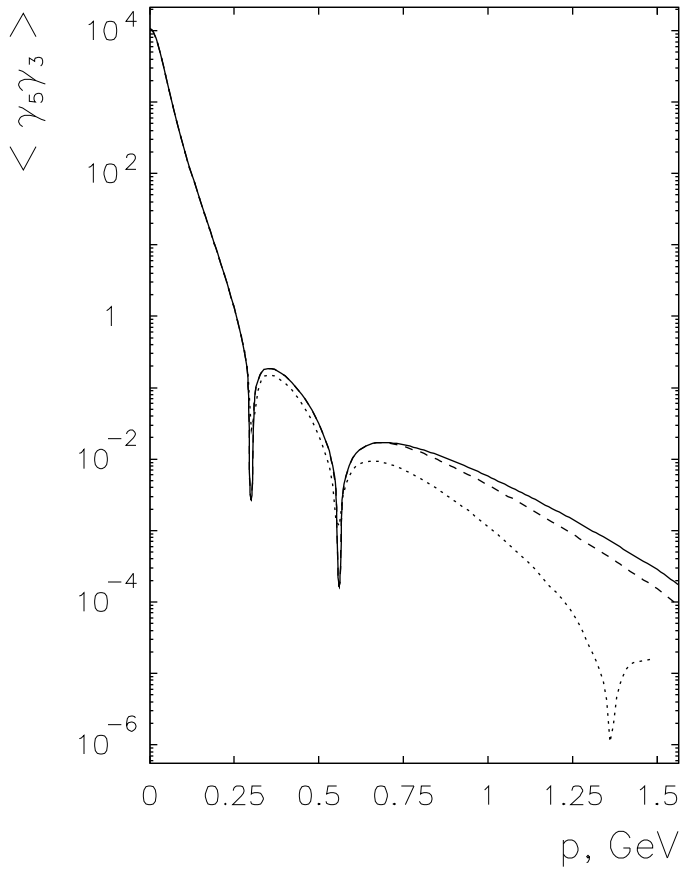
$< \gamma_5 \gamma_3 >$
10^4
10^2
1
10^{-2}
10^{-4}
10^{-6}
0
0.25
0.5
0.75
1
1.25
1.5
p, GeV

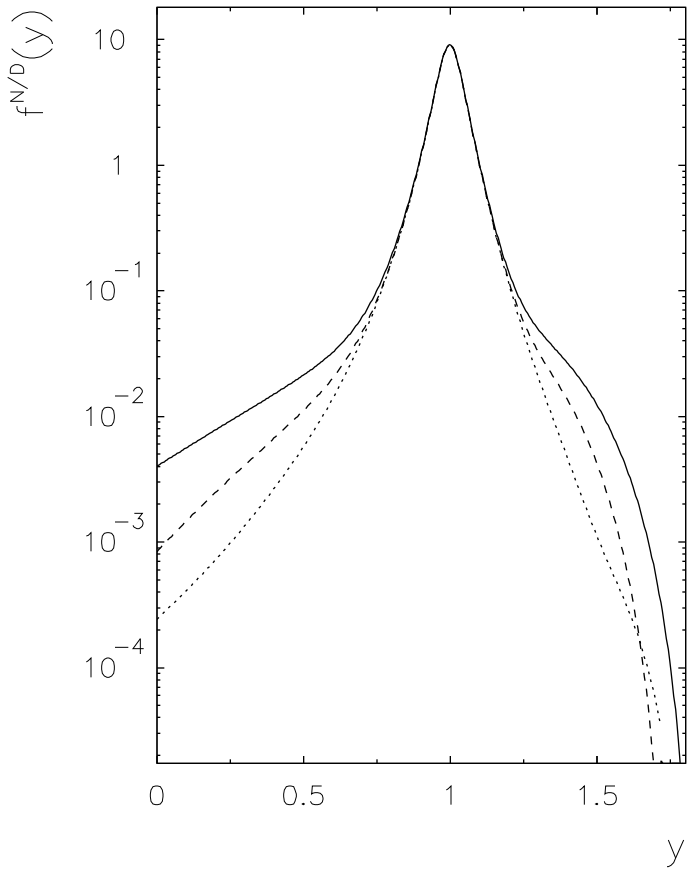
$f^{N/D}(y)$
10
1
10^{-1}
10^{-2}
10^{-3}
10^{-4}
0
0.5
1
1.5
y

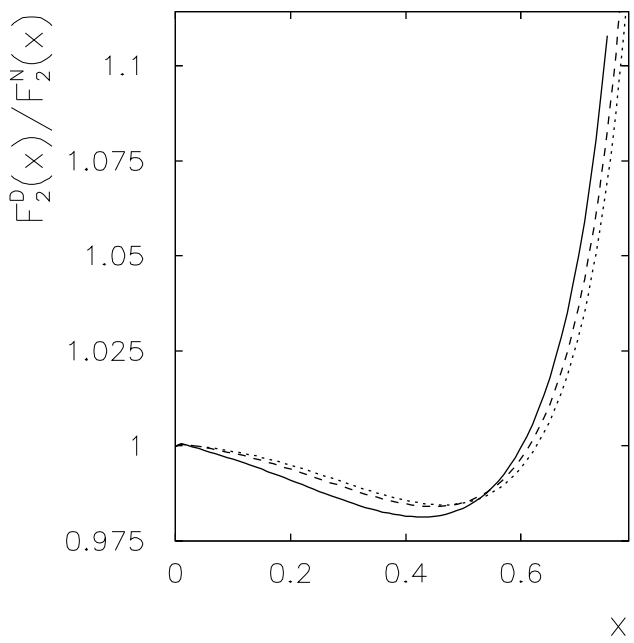
$F_2^D(x)/F_2^N(x)$
1.1
1.075
1.05
1.025
1
0.975
0
0.2
0.4
0.6
x

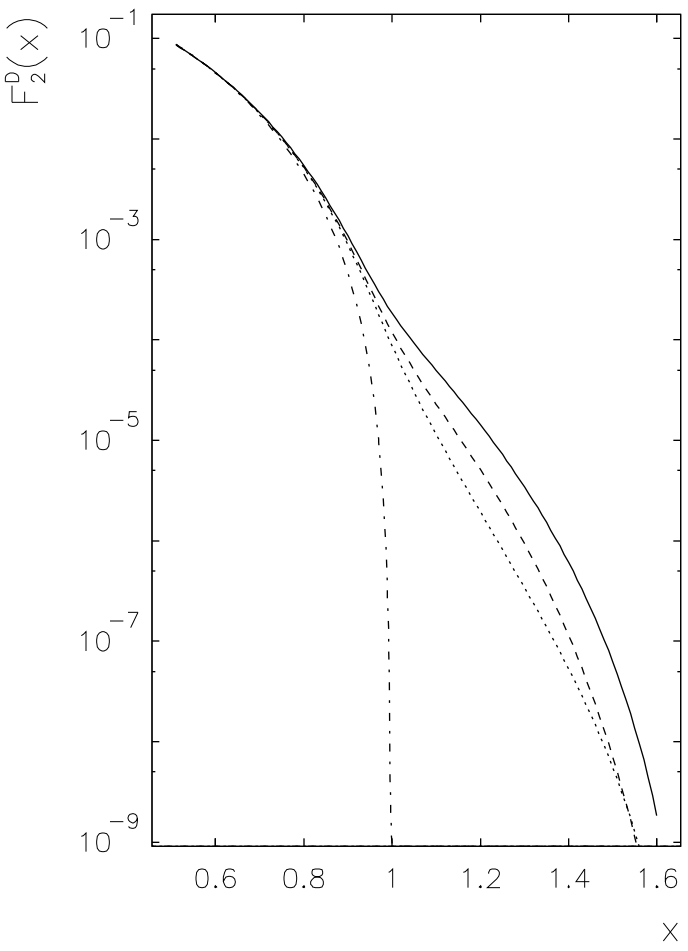
$F_2^D(x)$
10^{-1}
10^{-3}
10^{-5}
10^{-7}
10^{-9}
0.6
0.8
1
1.2
1.4
1.6
x

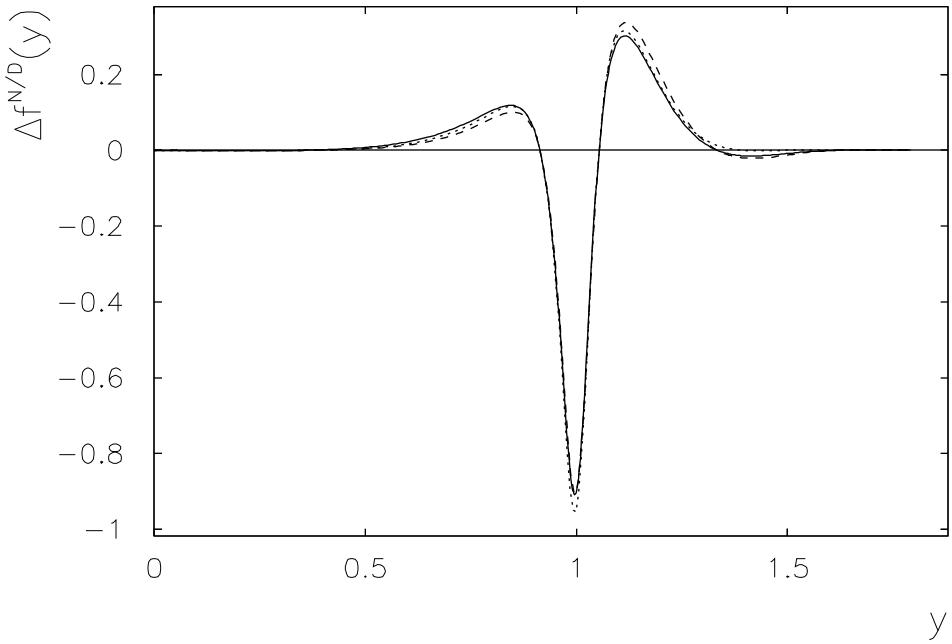
$\Delta f^{N/D}(y)$
0.2
0
−0.2
−0.4
−0.6
−0.8
−1
0
0.5
1
1.5
y

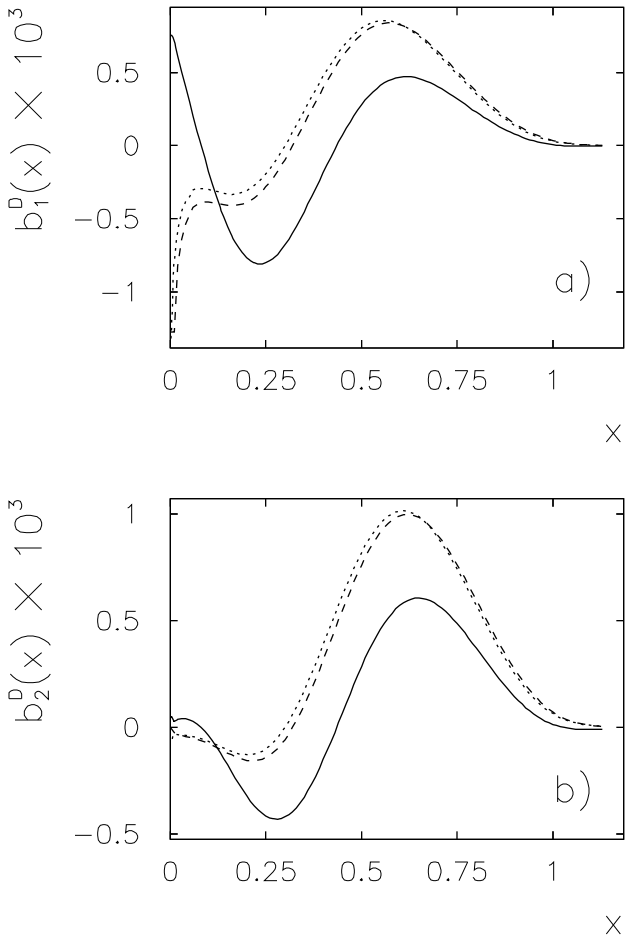
$b_1^D(x) \times 10^3$
0.5
0
−0.5
−1
a)
0
0.25
0.5
0.75
1
x
$b_2^D(x) \times 10^3$
1
0.5
0
−0.5
b)
0
0.25
0.5
0.75
1
x

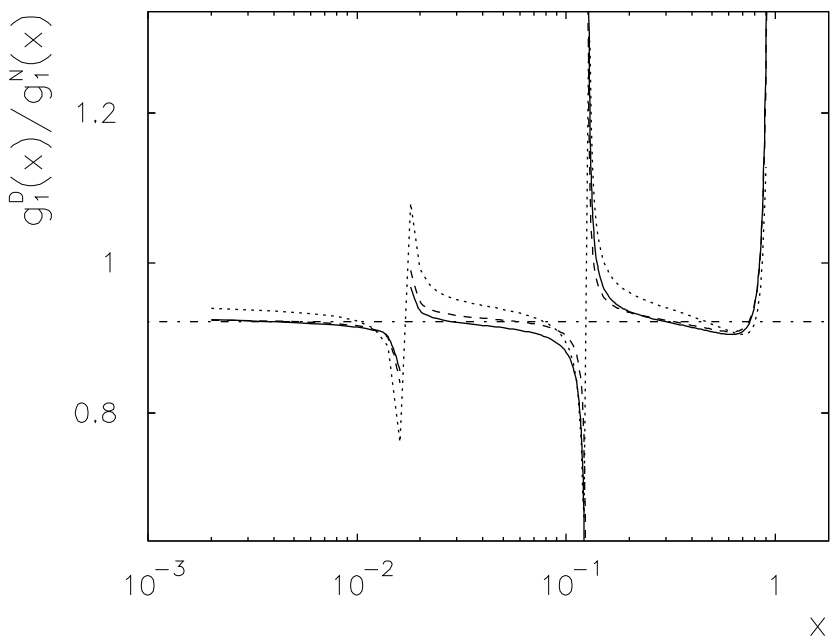
$g_1^p(x)/g_1^n(x)$
1.2
1
0.8
10^{-3}
10^{-2}
10^{-1}
1
x